AD-A167 885 DETERMINATION OF THE ATMOSPHERIC AEROSOL DISTRIBUTION BY MULTI-CHANNEL REMOTE SENSING TECHNIQUES(U) NAVAL POSTGRADUATE SCHOOL MONTEREY CA S R BULFINCH MAR 86 1/1

UNCLASSIFIED F/G 4/1 NL

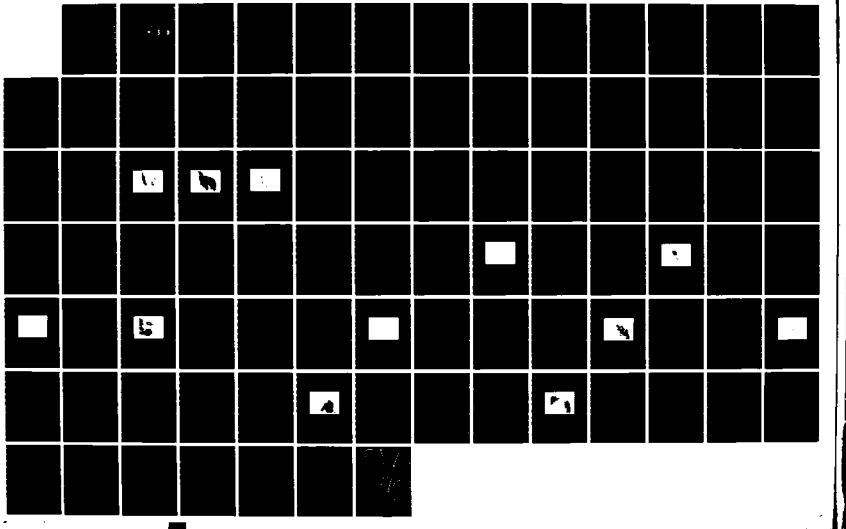

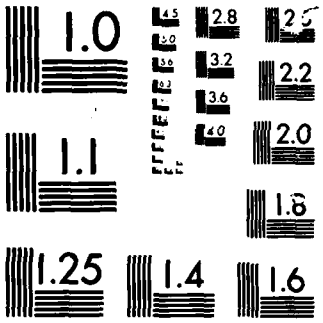

MICROCOPY CHART

NAVAL POSTGRADUATE SCHOOL
Monterey, California

THESIS

DETERMINATION OF THE ATMOSPHERIC AEROSOL DISTRIBUTION BY MULTI-CHANNEL REMOTE SENSING TECHNIQUES

by

Scott R. Bulfinch

March, 1986

Thesis Advisor: Philip A. Durkee

Approved for public release; distribution is unlimited.

SECURITY CLASSIFICATION OF THIS PAGE AD A167885

REPORT DOCUMENTATION PAGE

1a REPORT SECURITY CLASSIFICATION UNCLASSIFIED	1b. RESTRICTIVE MARKINGS
2a SECURITY CLASSIFICATION AUTHORITY	3 DISTRIBUTION / AVAILABILITY OF REPORT Approved for public release; distribution is unlimited.
2b. DECLASSIFICATION / DOWNGRADING SCHEDULE	
4 PERFORMING ORGANIZATION REPORT NUMBER(S)	5. MONITORING ORGANIZATION REPORT NUMBER(S)
6a. NAME OF PERFORMING ORGANIZATION Naval Postgraduate School 6b. OFFICE SYMBOL (If applicable) 63	7a. NAME OF MONITORING ORGANIZATION Naval Postgraduate School
6c. ADDRESS (City, State, and ZIP Code) Monterey, California 93943-5000	7b. ADDRESS (City, State, and ZIP Code) Monterey, California 93943-5000
8a NAME OF FUNDING / SPONSORING ORGANIZATION 8b. OFFICE SYMBOL (If applicable)	9. PROCUREMENT INSTRUMENT IDENTIFICATION NUMBER
8c ADDRESS (City, State, and ZIP Code)	10 SOURCE OF FUNDING NUMBERS PROGRAM ELEMENT NO. / PROJECT NO / TASK NO / WORK UNIT ACCESSION NO

11 TITLE (Include Security Classification)
DETERMINATION OF THE ATMOSPHERIC AEROSOL DISTRIBUTION BY MULTI-CHANNEL REMOTE SENSING TECHNIQUES

12 PERSONAL AUTHOR(S)
Bulfinch, Scott R.

13a TYPE OF REPORT	13b TIME COVERED	14 DATE OF REPORT (Year, Month, Day)	15 PAGE COUNT
Master's Thesis	FROM _____ TO _____	1986 March	88

16 SUPPLEMENTARY NOTATION

17 COSATI CODES			18 SUBJECT TERMS (Continue on reverse if necessary and identify by block number)
FIELD	GROUP	SUB-GROUP	Aerosol Distribution, Remote Sensing, Aerosol, Boundary Layer, Particle Distribution, Multi-Channel, AVHRR

19 ABSTRACT (Continue on reverse if necessary and identify by block number)

A simple image processing technique applied to channel 1 and channel 2 of the NOAA AVHRR sensor may be used to discern variations in aerosol particle size distribution. Ratios of the channel 1 albedo to the channel 2 albedo are calculated and displayed as an image. High ratio values are shown to indicate increased levels of submicron aerosols, while low ratio values indicate increased levels of supermicron aerosols. Horizontal variations in aerosol distributions may be observed directly by noting variations in ratio values, and vertical distributions may be inferred through the application of appropriate regional models of aerosol transport. A model of offshore advection of urban particles within the marine boundary layer is presented. Interpreting ratio values in light of this model, the offshore transport of urban aerosol particles is observed in AVHRR imagery of southern California during the period 17-25 October 1984.

20 DISTRIBUTION / AVAILABILITY OF ABSTRACT	21 ABSTRACT SECURITY CLASSIFICATION	
☒ UNCLASSIFIED/UNLIMITED ☐ SAME AS RPT ☐ DTIC USERS	unclassified	
22a NAME OF RESPONSIBLE INDIVIDUAL Philip A. Durkee	22b TELEPHONE (Include Area Code) 408-646-3465	22c OFFICE SYMBOL 63De

DD FORM 1473, 84 MAR 83 APR edition may be used until exhausted
All other editions are obsolete

SECURITY CLASSIFICATION OF THIS PAGE

Approved for public release; distribution is unlimited.

Determination of the Atmospheric Aerosol Distribution By Multi-Channel Remote Sensing Techniques

by

Scott R. Bulfinch
Lieutenant Commander, United States Navy
B.S., U. S. Naval Academy, 1970

Submitted in partial fulfillment of the
requirements for the degree of

MASTER OF SCIENCE IN METEOROLOGY AND OCEANOGRAPHY

from the

NAVAL POSTGRADUATE SCHOOL
March 1986

Author: 
Scott R. Bulfinch

Approved by: 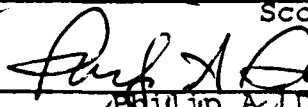
Philip A. Durkee, Thesis Advisor


Carlyle H. Wash, Second Reader

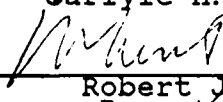
Robert J. Renard, Chairman,
Department of Meteorology


John N. Dyer,
Dean of Science and Engineering

ABSTRACT

A simple image processing technique applied to channel 1 and channel 2 of the NOAA AVHRR sensor may be used to discern variations in aerosol particle size distribution. Ratios of the channel 1 albedo to the channel 2 albedo are calculated and displayed as an image. High ratio values are shown to indicate increased levels of submicron aerosols, while low ratio values indicate increased levels of supermicron aerosols. Horizontal variations in aerosol distributions may be observed directly by noting variations in ratio values, and vertical distributions may be inferred through the application of appropriate regional models of aerosol transport. A model of offshore advection of urban particles within the marine boundary layer is presented. Interpreting ratio values in light of this model, the offshore transport of urban aerosol particles is observed in AVHRR imagery of southern California during the period 17-25 October 1984.

TABLE OF CONTENTS

LIST OF TABLES

LIST OF FIGURES

ACKNOWLEDGEMENTS

The completion of this study was made possible by the gracious assistance of many organizations and individuals. The Satellite Oceanography Facililty, Scripps Institution of Oceanography provided all NOAA-6 and NOAA-7 images and associated ephemeris data. Mr. J. Rosenthal of the Pacific Missile Test Center, Point Mugu Calif., provided collated buoy, surface and upper-air observations from which the meteorological analysis was largely drawn. Dr. James W. Fitzgerald provided San Nicholas Island sun photometer data from the Naval Research Laboratory SNI-84 experiment. Mr. Mike Gunning of the Department of Meteorology, U.S. Naval Postgraduate School provided invaluable assistance in all phases of computer programming and image processing. Finally, I would like to extend my thanks and appreciation to Professor Philip A. Durkee of the U.S. Naval Postgraduate School, without whose constant assistance, advice and understanding, this study would not have been possible.

I. INTRODUCTION

The ability of satellite-borne remote sensing instruments to detect variations in atmospheric aerosol particle concentrations has been documented by numerous investigators. The various meteorological satellites differ in their ability to discriminate between the relatively minor albedo variations attributable to variations in aerosol optical depth. Inasmuch as these sensors were not developed with aerosol investigation as a primary goal, attention must be paid to the limitations of each sensor, and sensor-specific techniques developed to optimize sensor capabilities in the aerosol-sensing mode. This investigation focuses on the NOAA-6 and NOAA-7 Advanced Very High Resolution Radiometer (AVHRR) and explores the capability of this sensor to discern variations in aerosol particle size distribution.

A. BACKGROUND

Knowledge of the variation of aerosol size distribution on a global basis may aid in the development of radiative transfer calculations in climate modeling. The inference of marine boundary layer relative humidity variations through the detection of boundary layer aerosol concentrations can aid in the study of marine boundary layer processes. However, such inferences are inhibited by the presence of free atmospheric aerosols above the boundary layer. When large concentrations of aerosols exist above the marine boundary layer, their contribution to total aerosol optical depth is proportionally greater, and thus the ability to infer boundary layer processes from aerosol concentration is limited.

In an experiment conducted off the Southern California coast in the vicinity of San Nicholas Island during the

early fall of 1982, boundary layer and free atmospheric aerosol composition and concentration data were acquired and compared to corresponding satellite images. The aerosol data were acquired in near real time in areas of observed brightness variations detected in images produced by the NIMBUS-7 Coastal Zone Color Scanner (CZCS) and the NOAA-7 AVHRR (Durkee et al., 1986). The results demonstrate a relationship between the size distribution of aerosols and the relative brightness counts measured by the NOAA-7 AVHRR channel 1 (red) and channel 2 (near-infrared); see also Durkee (1986). An earlier investigation in the western Atlantic Ocean showed a positive relationship between the aerosol size distribution as determined by AVHRR channels 1 and 2 and by sun photometer measurements taken aboard ship (Griggs, 1983).

While this study, and those cited above, have been limited in scope to the lower troposphere, analogous methods may be applied to investigate partical distributions at higher levels. Yue and Deepak (1983) have proposed a method for determining the size distribution of aerosols in the stratosphere by multi-channel techniques. The Yue and Deepak approach examines the difference in volume extinction coefficients for aerosols at 0.45 and 1.0 micron wavelengths and computes a ratio therefrom. By examining the results of the extinction of solar radiation at these wavelengths as sensed by the Stratospheric Aerosol and Gas Experiment (SAGE) instrumentation aboard NIMBUS-7, and applying appropriate models of stratospheric aerosol composition, the authors suggest a method to determine the spatial size distribution of the particles.

B. OBJECTIVES

This study returns to the vicinity of San Nicholas Island and exploits data acquired during the Naval Research Laboratory's Vertical Structure Experiment (SNI-84). NOAA-6

and NOAA-7 AVHRR passes occurring during the timeframe of the experiment are examined. Through comparison of satellite images with ground truth data, useful inferences of relative aerosol size distributions within and above the marine boundary layer are sought.

The primary objective is to examine the relationship between AVHRR channel 1 and channel 2 ratio values and changes in aerosol particle concentration. Ratio values are expected to increase as the relative concentration of smaller particles increase, and to decrease as the relative concentration of larger particles increase, thus serving as an indicator of aerosol size distribution.

Utilizing particle size distributions as determined by ratio values, inferences as to the vertical size distributions of aerosols are sought. Two models depicting the distribution of atmospheric aerosols in and above the boundary layer are considered. The ability to describe vertical variations in particle distribution based on AVHRR ratio values is shown to depend on the model assumed for a given locality.

The extraction of meaningful relationships with a minimum of image processing is a secondary objective. A COMTAL image processor in consort with a VAX 11/780 computer system was utilized in the analysis of images acquired during the experiment. The amount and sophistication of processing was deliberately minimized in the interest of establishing a compact, operationally useful technique.

C. ORGANIZATION

In Chapter II, the theory of atmospheric aerosol particle composition, its origin and distribution is presented. A model for the transport of terrestrial aerosols above the boundary layer is presented and limitations of the model discussed.

In Chapter III, the image processing and data analysis procedures are described. Chapter IV presents the analysis results and discussion of findings. Each day of the experiment on which useful imagery was acquired is examined in detail. In Chapter V, conclusions drawn from the analysis are summarized.

II. PROCESSES AND THEORY

A. PARTICLE CHARACTERISTICS

1. Boundary Layer Particles

Aerosol particles within the marine boundary layer normally consist of the evaporative residue of bursting seawater bubbles, and thus possess nuclei of soluble sea salts. Being water soluble, these particles may be expected to respond to changes in relative humidity within the marine boundary layer. Durkee et al., (1986) have shown that, for the 1982 experiment region, variation in relative humidity within the boundary layer is the dominant mechanism for producing variation of upwelling radiance, although wind speed variations can also be important. The marine particle size distribution varies directly with the relative humidity. Thus, in a humid marine boundary layer environment, a proportionally greater number of larger particles may be expected than in the free troposphere above the boundary layer.

Shettle and Fenn (1979) have modeled the variation in size distribution of marine aerosols with relative humidity. Fig. 2.1 shows that as relative humidity increases, the number of particles of all sizes increases. However, it is apparent from Fig. 2.1 that the relative increase in number of particles at a given radius for a given increase in relative humidity is greater for the larger, supermicron (> 1.0 micron) particles than for smaller, submicron (< 1.0 micron) particles.

2. Upper-Level Particles

Aerosols occurring in the free troposphere above the marine boundary layer are composed of a mix of particle types, principally of marine (salt), rural (soil/dust) and urban (soot) origin. In a stable, cloud-free atmosphere,

these particles reside in a regime of much lower relative humidity than do boundary layer particles. They are also less hygroscopic due to their composition. As a result, upper- level aerosols may be expected to consist of a proportionally greater number of smaller particles than boundary layer aerosols. A mechanism for the formation of significant numbers of upper-level particles was presented by Durkee et al.,(1986) and is depicted in Fig. 2.2. In this model, radiative heating over land areas, with associated convective lifting, allows terrestrial particles to rise above the level of the marine boundary layer. Once above the boundary layer, the particles spread out laterally under the effect of a stable upper-level subsidence regime.

B. DETECTION OF UPPER-LEVEL PARTICLES

1. Wavelength Dependence of Aerosol-Influenced Radiance

It has been shown by Durkee (1986) that for particles of urban and rural origin, single scattering albedo w_o, scattering phase function $p(\Theta)$ and aerosol optical depth τ, the aerosol-dependent terms in the radiative transfer equation, are larger at red wavelengths than at near-infrared wavelengths. These parameters remain relatively constant with wavelength for marine particles.

Since radiance, L, is approximately proportional to single scattering albedo, scattering phase function and optical depth, variations in radiance may be related to variations in the aerosol dependent terms. Applying the calculations at red and near-infrared (NIR) wavelengths, a simple ratio may be formed:

$$\frac{L(\text{red})}{L(\text{nir})} \propto \frac{(w_o\ p(\Theta)\ \tau)\text{red}}{(w_o\ p(\Theta)\ \tau)\text{nir}} \qquad (2.1)$$

This ratio will be larger in the presence of increased concentrations of small particles, due to the

short-wavelength bias of the small particles. Where particle size may be related to a vertical distribution of particles, such as in the model depicted by Figure 2.2, the ratio will lead to inferences of the relative vertical distributions of particles.

2. AVHRR Exploitation of Aerosol Wavelength Dependence

The NOAA-6 and NOAA-7 are sun-synchronous, polar orbiting satellites. Each orbiter makes one daylight pass over the southern California area per day: NOAA-6 makes a descending (decreasing north latitude) pass in the morning and NOAA-7 makes an ascending (increasing north latitude) pass in the mid-afternoon. During the experiment period, the NOAA-6 orbiter's morning pass varied from 0800 to 0830 Pacific Daylight Time (PDT), while the NOAA-7 orbiter's afternoon pass varied from 1530 to 1700 PDT. Those days on which images from both orbiters were obtained provided excellent opportunities to examine diurnal processes.

Channel 1 of the NOAA-6 and NOAA-7 AVHRR responds to radiance in the red wavelength; channel 2 to that in the near-infrared (see Fig. 2.3). Radiance measured by channels 1 and 2 thus may be expected to vary with the terms discussed above. Specifically, for upper- level particles, a ratio of channel 1 radiance to channel 2 radiance will be larger than the same ratio applied in the absence of upper-level particles.

The validity of this method was demonstrated by Durkee (1986). Actual measurements of upper-level and boundary layer particles were taken and the relative contribution of each to total optical depth calculated. The optical depth calculations showed excellent correlation with AVHRR channel 1 / channel 2 ratios. Fig. 2.4 demonstrates the agreement between ratios of calculated optical values and ratios obtained from multichannel sensor measurements during the 1982 experiment. Note how both calculated and

observed values exhibit the same behavior following a frontal passage. Prior to frontal passage, all ratio values are high. This corresponds to the presence of significant concentrations of small particles above the boundary layer. Following frontal passage, all ratio values are observed to decrease. This effect is due to fewer smaller particles in the lower troposphere after passage of the front.

C. LIMITATIONS OF PARTICLE DISTRIBUTION HYPOTHESIS

1. Barriers to Convective Mixing

The mechanism depicted in Fig. 2.2 depends on convective lifting to disperse terrestrial aerosols above the boundary layer. This implies a certain level of instability in the lower troposphere. Radiative heating of the land surface is the dominant process for production of the instability shown. Where such instability is not present, the transport of boundary layer particles into the free troposphere will be inhibited.

2. Terrestrial Particles in the Boundary Layer

In coastal regions subject to excessive emissions of rural or urban particles into the atmosphere, the assumption that boundary layer aerosols consist primarily of marine particles may not be valid. Where a capping inversion is common, and where particle sources are beneath the inversion, a complex mixture of urban and rural particles may be largely trapped within the boundary layer. These particles will be advected for considerable distances offshore with the prevailing winds.

Such a mixture of particles will exhibit an exceedingly complex range of solubilities and hygroscopic properties. Therefore the particles will respond unpredictably to variations in boundary layer relative humidity.

When high concentrations of terrestrial particles are present in the marine boundary layer, the relationship expressed in eqn. 2.1 may not directly relate to

concentrations of upper-level particles. An occurrence of the apparent advection of urban aerosols over the contiguous waters of southern California will be examined in Chapter IV.

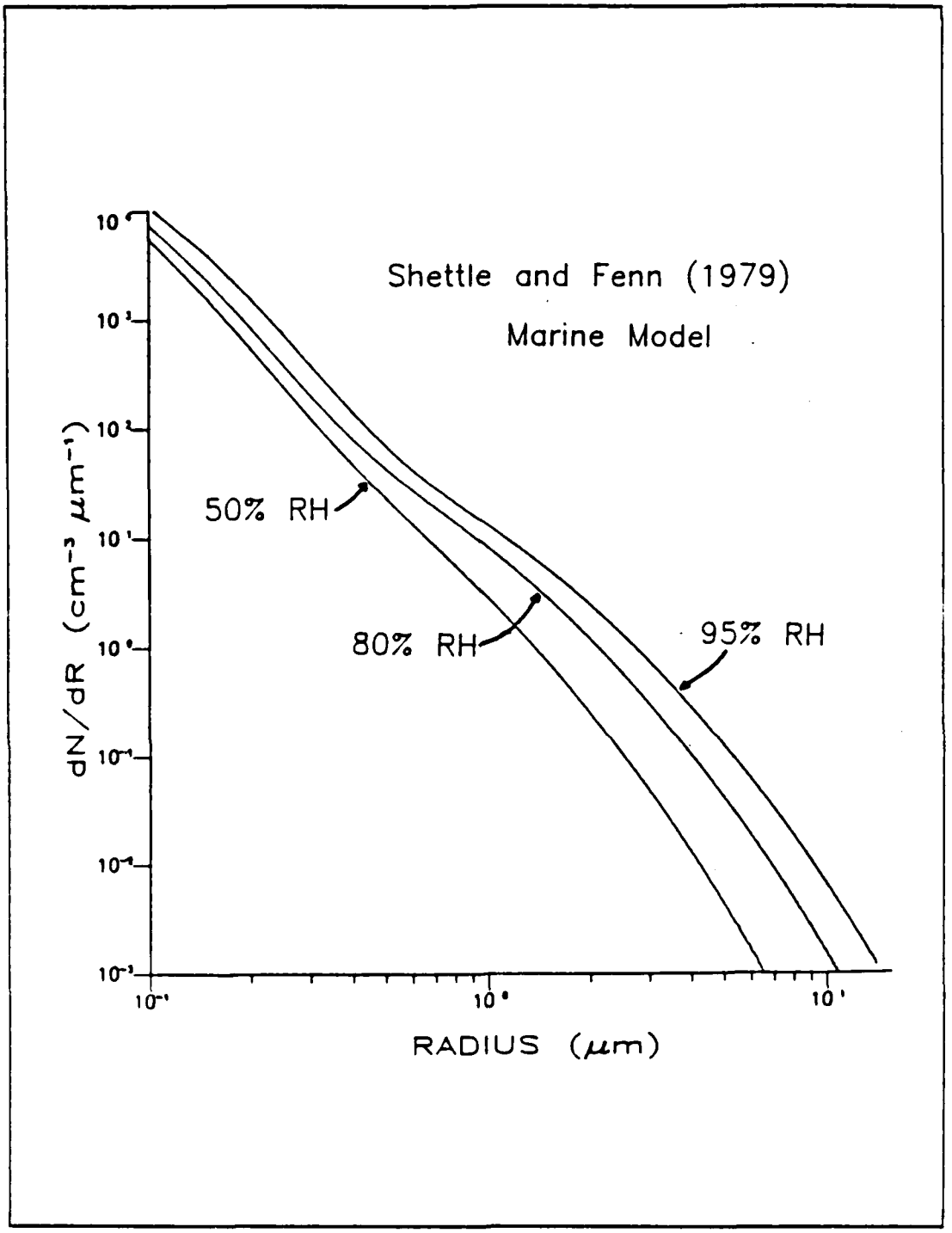

Fig. 2.1 Variation of the marine model size distribution of Shettle and Fenn (1979) with relative humidity.

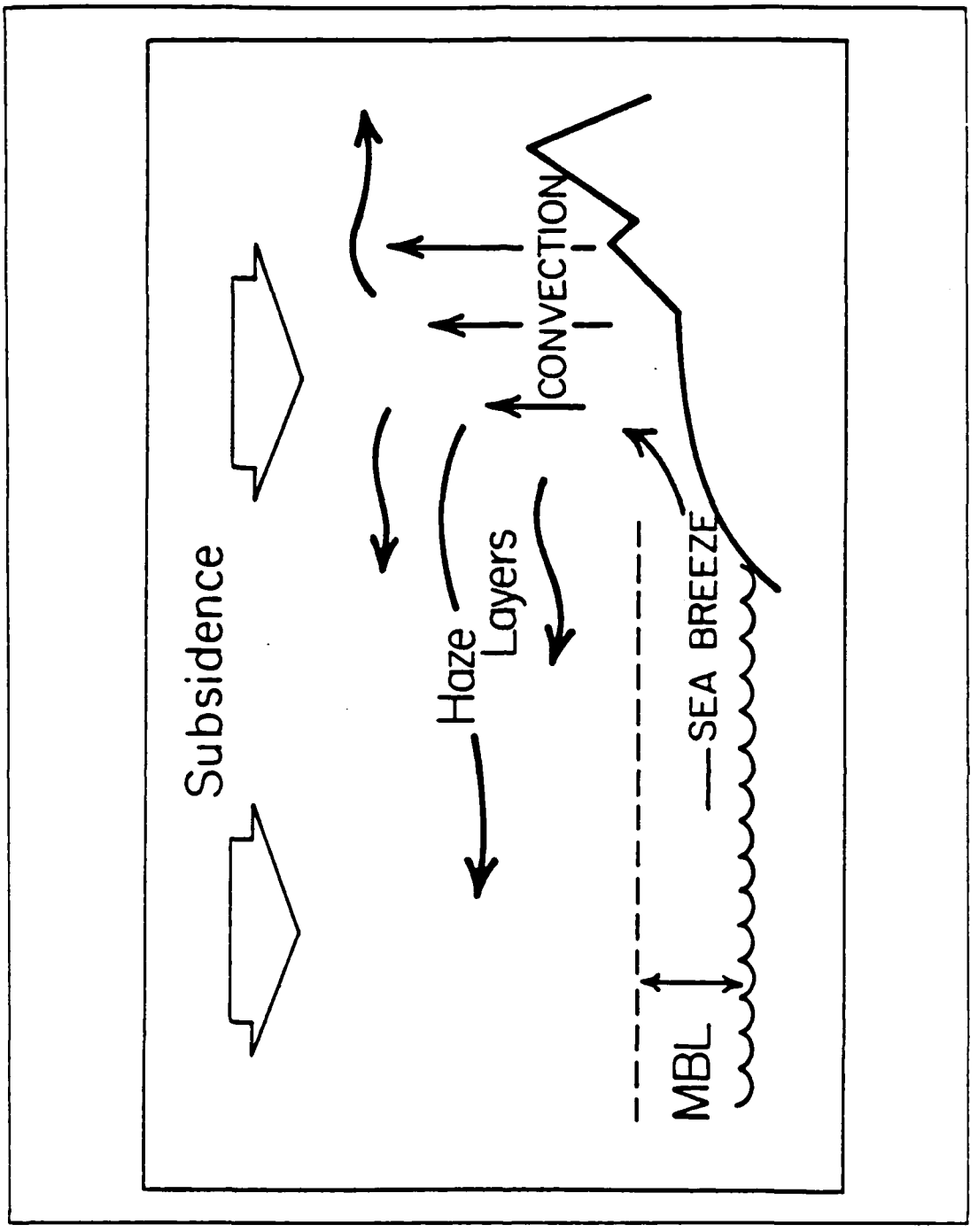

Fig. 2.2 Mechanism for the formation of significant layers of small particles above the boundary layer (from Durkee 1986).

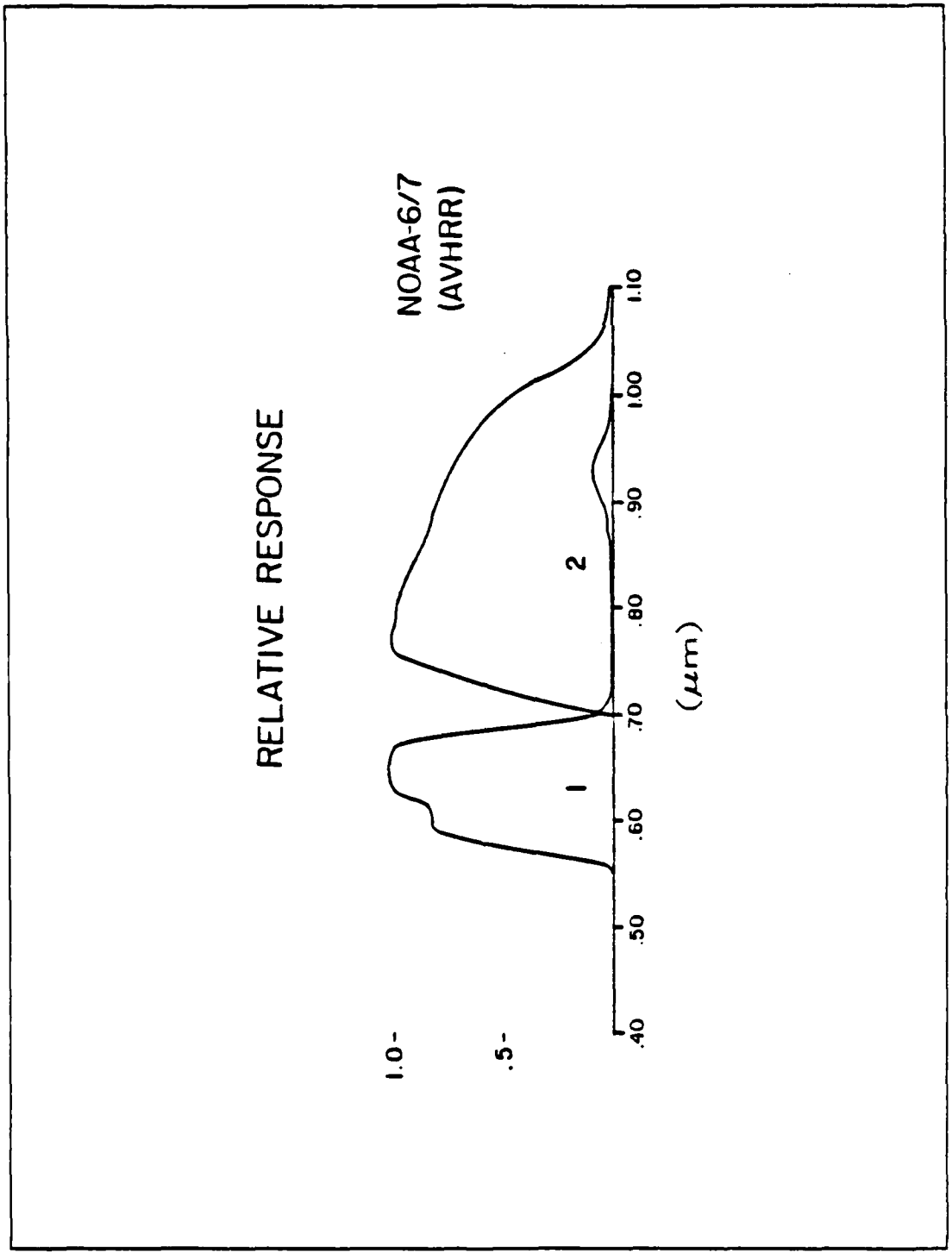

Fig. 2.3 Spectral response of AVHRR channels 1 and 2.

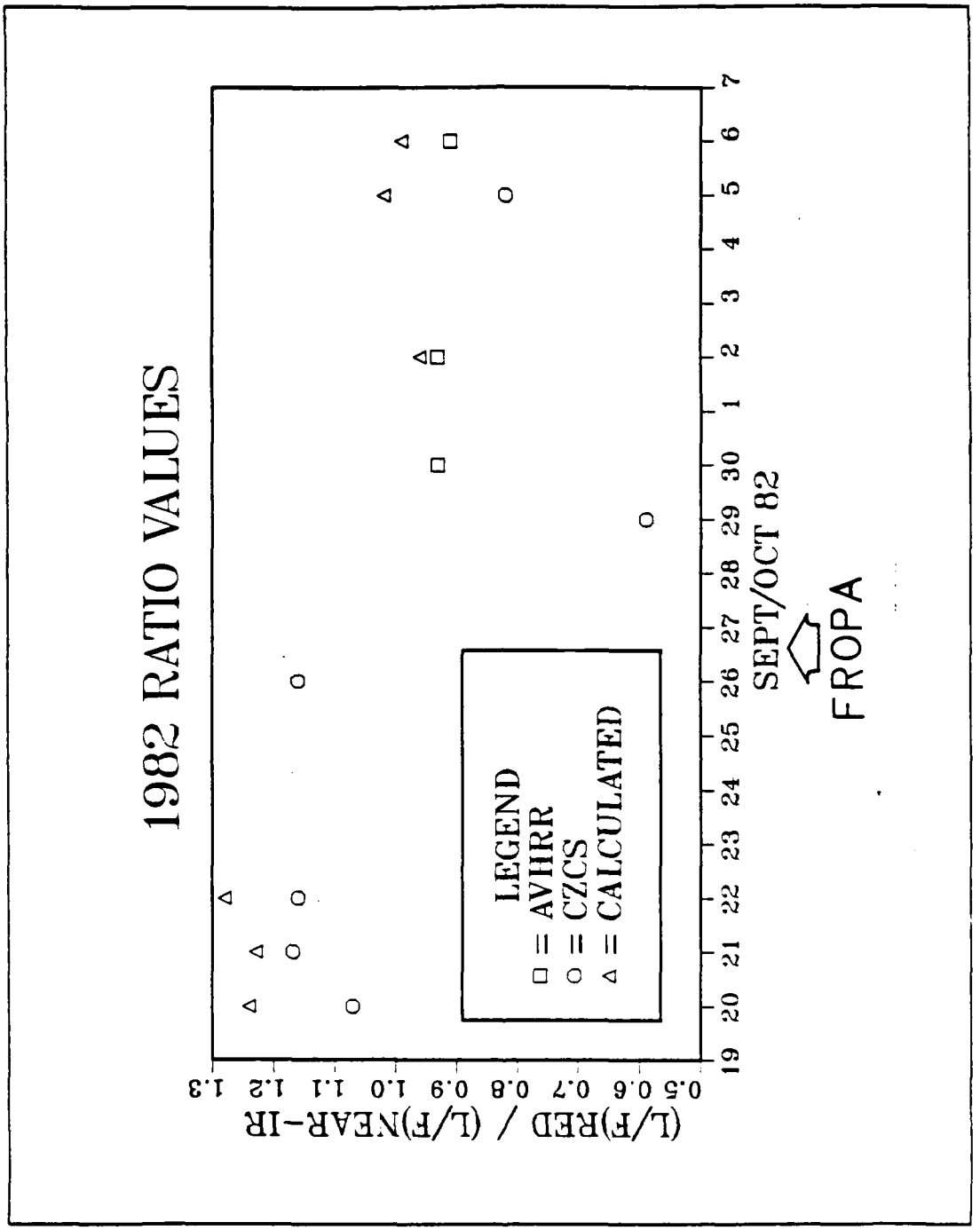

Fig. 2.4 Changes in satellite-detected and aircraft-measured ratio values following frontal passage (from Durkee, 1986).

III. PROCEDURES

A. RELATING AVHRR CHANNEL 1 AND CHANNEL 2 BRIGHTNESS COUNTS

1. Conversion of Brightness Counts to Albedo

The AVHRR sensor images are depicted as digital brightness count integers. As discussed by Lauritson et al., (1979), values of albedo may be obtained from the brightness count according to the relation:

$$A = G X + I \qquad (3.1)$$

where A is albedo in percent, X is the brightness count and G and I are calibration coefficients. The values of G and I for the AVHRR are presented in Table I

TABLE I

Values of G and I for the AVHRR Sensor Channels 1 and 2

(From Lauritson et al., 1979)

	G	I
Channel 1	0.1068	-3.44
Channel 2	0.1069	-3.488

2. Processing of Image Ratios

Albedo values for each image pixel of the AVHRR channel 1 and channel 2 were calculated utilizing the relationship of equation 3.1 for each image pixel. The ratio of the albedos was then calculated pixel by pixel to produce an image of ratioed albedo values. These values were normalized by a factor of 100 so as to fall in the range of 0-255 for processing on the COMTAL image processing system.

The range of ratio values for a given image was typically small. Therefore, a stepped transfer function was applied to the ratioed image to enhance ratio variations for

ease of interpretation and display. The enhancement function provided fourteen gray shades corresponding to ratio values in increments of 0.05 in the range 1.20 to 1.90 (see Table II), running dark to light. Gray shades are equivalent from image to image. Significant brightness, and hence ratio values, are labelled on each image to aid in image interpretation.

TABLE II

Enhancement gray shades

Gray Shade #	Range of Values
1	1.20--1.24
2	1.25--1.29
3	1.30--1.34
4	1.35--1.39
5	1.40--1.44
6	1.45--1.49
7	1.50--1.54
8	1.55--1.59
9	1.60--1.64
10	1.65--1.69
11	1.70--1.74
12	1.75--1.79
13	1.80--1.84
14	1.85--1.89

Examples of a channel 1 image, a channel 2 image, and the multi-channel ratio image for one pass of NOAA-6 are shown in Figs. 3.1 through 3.3. The stepped enhancement function was not applied to the single channel images. The range of brightness values on these images was extremely small; hence separate enhancements were applied to aid in display.

B. CLOUD CONTAMINATION

The techniques of this investigation are limited in application to a cloud-free atmosphere. In order to confirm areas of cloudiness, particularly thin cirrus, AVHRR channel 4 images were examined as well as the raw (unratioed) channel 1 and channel 2 images. Clouds appear as dark signatures on the ratio images. This is due to the fact that the ratio technique responds to the change in relative

particle concentrations between submicron and supermicron particulate aerosols. When the difference in relative concentrations decreases, either due to a decrease in submicron particles or an increase in supermicron particles, the ratio value becomes smaller, and hence darker under the display convention in use. A 1.2:1 ratio (or smaller) appears black. Thus, the relatively large cloud droplets produce areas of low ratio.

C. ATMOSPHERIC VARIABLES

The AVHRR ratio images were examined and compared to measured local synoptic conditions and surface aerosol concentrations. Mack et al., (1985) provide a comprehensive collection of meteorological variables measured at San Nicholas Island during the timeframe examined. The aerosol concentrations presented by Mack et al.,(1985) are derived from twenty-minute averages, tabulated hourly. A variety of particle sensing instruments were used to sample aerosols of varying size. Measurements of aerosols represent surface concentrations only; no measurements were obtained above the boundary layer. Aerosols of 0.01 to 1.0 micron diameter were measured with a Thermo-Systems Electrical Aerosol Analyzer Model 3030. Aerosols of 0.5 to 10 micron diameter were measured with a Royco Model 225 Optical Particle Counter. Where a transition from one instrument to another occurs, at 0.5 to 1.0 micron, a discontinuity is normally seen in the data. The reader is referred to Mack et al., (1985) for a description of the particle data acquisition system.

Sun photometer data acquired by the Naval Research Laboratory during certain portions of the experiment period at San Nicholas Island were examined. The sun photometer provides a measure of aerosol optical depth, τ, at selected wavelengths. Measured values of τ at 0.64 microns and 0.88 microns were ratioed and the resulting value compared to AVHRR channel 1 and channel 2 ratio values.

Hourly synoptic data from NOAA automated data buoys 46023, 46024, and 46025, and from San Nicholas Island itself were examined. Surface wind data extracted from the synoptic records are presented graphically on the images displayed in Chapter IV. The wind data depicted represent a 3-hour average of wind speed and direction for the three hours immediately preceding image time. Rawinsonde sounding data from San Nicholas Island were utilized to evaluate moisture levels in the lower troposphere.

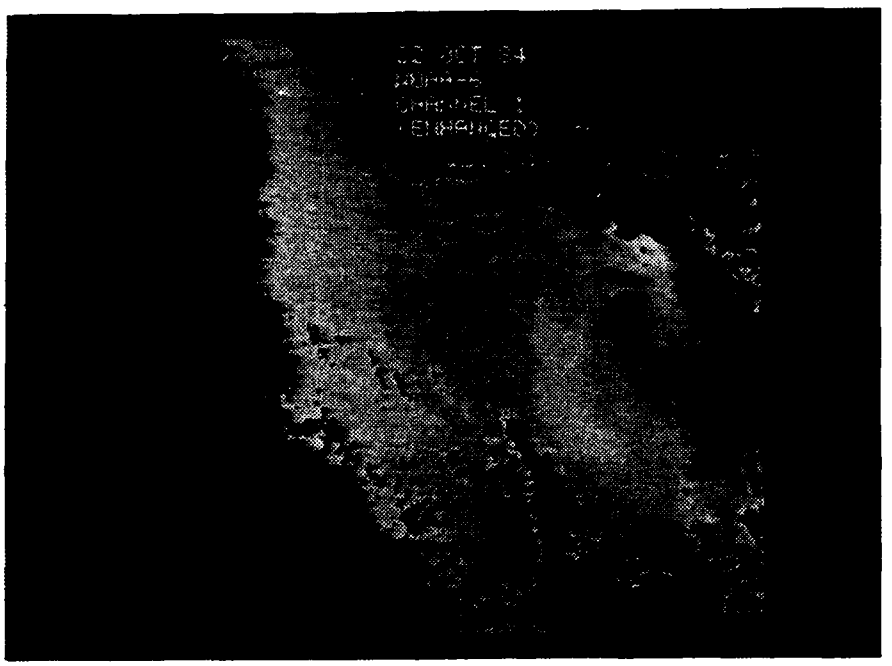

Fig. 3.1 NOAA-6 Channel 1 enhanced image
22 October 1984.

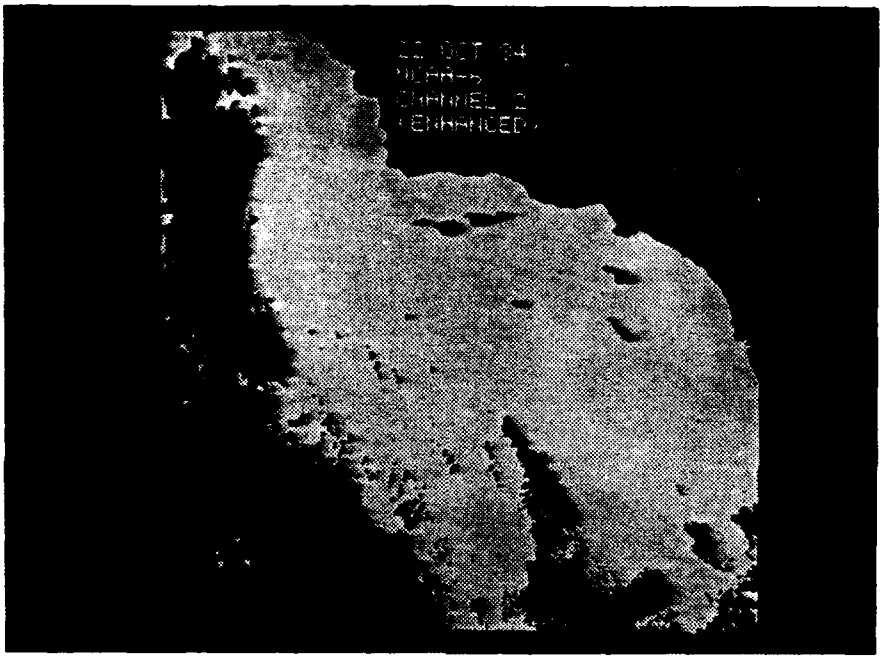

Fig. 3.2 NOAA-6 Channel 2 enhanced image 22 October 1984.

Fig. 3.3 NOAA-6 Channel 1 / Channel 2 ratio image, 22 October 1984.

IV. RESULTS AND DISCUSSION

An analysis of satellite data and meteorological variables obtained for the period of 17 to 25 October 1984 is presented in this chapter. Relationships are sought between relative magnitudes of AVHRR channel 1 and channel 2 ratio values and corresponding measurements of relative humidity, aerosol particle concentration and optical depth. AVHRR ratios calculated in close proximity to San Nicholas Island are compared to sun photometer measurements of optical depth at appropriate wavelengths. Due to intermittent cloud obscuration of San Nicholas Island, comparisons of image data to ground truth measurements cannot be made for every day of the experiment. During one two-day period, a significant instance of offshore advection of aerosols was noted; this period is examined in detail.

This study seeks to extend an investigation of the multi-channel ratio technique suggested in the southern California experiment described by Durkee (1986). Particle concentrations are seen to respond in a predictable and expected manner to changes in relative humidity. It will also be shown that ratio values readily indicate the variation in size distribution of aerosols.

A major frontal passage occurred during the time period examined by Durkee (1986), sharply altering the air mass characteristics off the coast of southern California. No such event occurred in SNI-84; hence, a time series of AVHRR channel 1 and channel 2 ratio values does not display any dramatic changes such as those noted by Durkee (1986).

Fig. 4.1 depicts NOAA-6 and NOAA-7 ratio values recorded in the vicinity of San Nicholas Island during the experiment period. Cloud cover and data availability limited the number of days to those shown. NOAA-7 ratio values are

shown to be lowest on the 17th and 18th of October; a substantial disparity exists between NOAA-6 and NOAA-7 on the 18th. This disparity is possibly due to sun-glint contamination of the NOAA-7 data, and will be discussed below. Ratio values are somewhat higher later in the experiment, with nearly equal values obtained from NOAA-6 and NOAA-7 on the 22nd.

A. METEOROLOGY

During the period of 17 through 25 October 1984, the large scale weather pattern of southern California and contiguous waters was dominated by the Eastern Pacific Ocean subtropical ridge. On 17 and 18 October, prevailing winds were northwesterly, and the experiment area was occupied by a marine air mass. On the 19th of October, a weak, non-precipitating surface trough moved rapidly through the area, accompanied by a wind shift to a more westerly component, and by low overcast. Moisture levels on the 19th were the highest recorded during the experiment. The high moisture levels were accompanied by a sharp drop in the concentrations of small aerosol particles. At the same time, high levels of large particle concentrations were observed. On 20 October, winds increased and again became northwesterly. On the 21st of October, thermal troughing over the southwestern United States / Baja California region intensified, accompanied by a decrease in intensity of the northwesterly winds at San Nicholas Island. No image data were available for the 20th and 21st.

On the 22nd and 23rd of October 1984, a marked change in the local circulation in the southern California region occurred. The prevailing light northwesterly winds were overcome by a northeasterly offshore component, typically becoming established in early- to mid-morning and sustained until mid-afternoon. From NOAA environmental buoy measurements, as well as San Nicholas Island observations, this

offshore flow appears to have been sustained to a distance of 125-150 km seaward from the California coast. The impact of this low-level offshore wind component on the offshore transport of aerosols from the Los Angeles metropolitan area will be examined later in this chapter. Fluctuations of particle concentrations for both large and small particles was noted throughout the day. The fluctuations are believed to relate to the passage of a plume of low-level urban / terrestrial aerosols over San Nicholas Island. Sounding data from the 23rd showed a marked drying in the lower troposphere, which was accompanied by a sharp drop in the concentration of large aerosol particles, and an attendant rise in the numbers of small particles.

On 24 October 1984, the mid-day offshore component largely vanished, as offshore winds became predominately west-northwesterly. Surface-layer moisture levels were re-established to near normal levels for the experiment period, while the free atmosphere remained relatively dry. Large particle concentrations were again low throughout much of the day, while no significant changes were noted in small particle concentrations. On October 25th, light offshore flow was again evident, although not as intense as on the 22nd and 23rd. Large particle concentrations remained relatively constant throughout the day, with the levels of small particles showing an increase. Cloud cover precluded the calculation of ratio values near San Nicholas Island.

A diurnal behaviour in particle concentrations was noted throughout the experiment period. In general, small particles underwent a net increase from morning to afternoon on each day, while large particles experienced a net decrease. Specifically, large particles were noted to decrease in number by the late afternoon on every day except the 25th (behavior of all particles on the 17th being unspecified, as no morning measurements were available). On the 25th, large

particles remained relatively constant in concentration. On the 19th, under the influence of significantly increased moisture levels, small particles showed a diurnal decrease; otherwise they remained fairly constant or showed increases throughout each day.

B. 17 OCTOBER 1984 CASE

NOAA-7 imagery for the 17th of October 1984 presents the lowest ratio values encountered in the study, ranging from low values of 1.21 to 1.24 in open ocean areas to high values of 1.30 to 1.35 near the coast (see Fig. 4.2). Moderate west to northwesterly winds predominate throughout the region, with typical values of 320 deg, 17 kt being recorded at San Nicholas Island near imaging time. Rawinsonde data show a stable, relatively dry lower troposphere above the marine boundary layer; the most stable sounding noted during the period of investigation (see Fig. 4.4). Particle concentrations (see Fig. 4.3) show moderate levels of supermicron particles, and relatively low levels of submicron particles. In the vicinity of San Nicholas Island, a mean ratio value of 1.25 is noted. The ratio of optical depth at .64 microns to optical depth at .88 microns as measured by the sun photometer is 0.94. The particulate distribution is expected for a typically moist marine boundary layer. Further, the satellite and photometer ratio values observed, which are low for the experiment period, demonstrate the expected response to the particle concentrations.

Late on the 16th of October 1984, a weak, non-precipitating frontal feature moved through the southern California area. No data exist prior to the 17th with which to confirm the state of the lower atmosphere at that time. However, earlier investigations (Durkee, 1986) have demonstrated a drop in small particle concentrations associated with a marine frontal passage. Thus, the values noted on

the 17th are not inconsistent with expected behaviour, and the low ratio values throughout the image are consistent with the particle concentrations. However, it must be pointed out that satellite geometry for NOAA-7 on the 17th of October was such that sunglint contamination of the image is a possibility. Recalling the relationship of equation 2.1, the ratio technique depends on the relationship:

$$\text{Albedo(red)} \;/\; \text{Albedo(nir)}$$

When sunglint effects are added to this relationship, a new relation results, specifically:

$$\text{Albedo(red)} + A(g) \;/\; \text{Albedo(nir)} + A(g)$$

where A(g) represents the upwelled albedo due to sunglint, which is essentially equal for both red and near-infrared wavelengths. As the value of A(g) increases, the value of the entire ratio is seen to approach unity. Thus, the net effect of sunglint contamination is to decrease any ratio of red to near-infrared radiance which is greater than 1.0. Therefore, conclusions drawn from the lower ratio values on the 17th must be viewed with caution.

A technique for estimating the contribution of sunglint to upwelled radiance is described by McClintock et al., (1971). Utilizing this technique, which characterizes surface roughness as a function of wind speed, it should be possible to estimate the contamination of an image by sunglint. Although not accomplished in this study, application of the McClintock et al. process in future studies should improve the ability to discern variations in aerosol concentrations.

C. 18 OCTOBER 1984 CASE

The 18th of October 1984 represents one of two days in this study on which imagery from both NOAA-6 (morning) and NOAA-7 (afternoon) are available. The NOAA-6 ratio image

shows a dramatic rise in values from those encountered the previous day via NOAA-7 (see Fig. 4.5). Ratio values range from highs of 1.85 in open ocean areas to lows of 1.63 near the coast. Note two plumes of low-ratio values emanating seaward from the southern California coast (A and B). Wind reports taken from NOAA data buoy 46025, located to the northeast of San Nicholas Island, indicate a period of light, north-northeasterly offshore flow from 1200 to 1900 GMT. These low-ratio features represent the seaward advection of urban and terrestrial aerosols in response to the offshore flow.

At San Nicholas Island, winds were light and northwesterly throughout the day. Morning particle concentration measurements indicate a substantial rise in small particle concentrations from those recorded on the previous afternoon (see Fig. 4.6). These increased levels of small particles support the increase in channel 1 / channel 2 ratio values over those values observed on the 17th by NOAA-7. The ratio value near San Nicholas Island is 1.80. By comparison, the ratio of optical depths as measured by sun photometer is 1.43. Rawinsonde data (Fig. 4.7) recorded at 2113 GMT shows a relatively dry lower troposphere, with a particularly dry layer between 800 and 900 mb. However, note the layer of increased moisture between 600 and 500 mb. This feature is a precursor of the weak weather system which will appear on the 19th.

NOAA-7 imagery recorded in the afternoon reveals a substantial decline in ratio values (see Fig. 4.8). The ratio value recorded at San Nicholas Island was 1.32; the sun photometer ratio was 1.26. From Fig. 4.9, it is evident that small particles increase in concentration throughout the day, while large particles decrease. This apparent discrepancy from the expected changes indicated by the changing ratio values during the day leads to the

consideration of potential contamination of NOAA-7 data by sunglint. The NOAA-7 geometry for 18 October is similar to that of the 17th. The channel 1 / channel 2 ratio values noted are inconsistent with the behavior of the particle concentration levels. It cannot be discounted that the ratio values are responding to particle distributions at levels above the surface detection instruments, but there are no indications that such is the case.

D. 19 OCTOBER 1984 CASE

On the 19th of October 1984, a weak lower-level perturbation moved through the area, bringing substantial cloud cover to southern California waters, and obscuring San Nicholas Island during satellite viewing times. In those few open areas visible through the clouds, NOAA-7 ratio imagery indicates a substantial rise in ratio values from those noted in the two previous days. Of note is the fact that earth-satellite geometry for NOAA-7 on the 19th eliminates the possibility of sunglint contamination. Ratio values recorded on the 19th range from 1.70 to 1.81 (see Fig. 4.10).

Rawinsonde data recorded at 1534 GMT, approximately three and one- half hours prior to image time, shows the expected moist sounding; the highest moisture levels encountered during the study (see Fig. 4.11). A comparison of Fig. 4.12 and Fig. 4.13 reveals that concentrations of all particles decrease during the day, but that submicron particles decrease dramatically, to levels nearly an order of magnitude less than those of the previous day. This is an expected response to the moist environment of the 19th. Review of surface weather observations at San Nicholas Island on the 19th indicates broken middle and high cloudiness in the morning, becoming overcast low clouds near noon. Significantly, the hourly particle concentration measurements show rapid decreases in the concentrations of

submicron particles nearly coincident to the onset of low cloudiness, which is the expected relation. Since no satellite or photometer ratio values are observable in the vicinity of the particle measurements at San Nicholas Island, it is difficult to draw conclusions regarding the ratio behavior. However, in those few cloud-free areas in which ratios may be observed, their values tend to be higher than the low levels of submicron particles would suggest. This may represent the remnants of areas of high submicron particle concentrations noted in prior observations, and may not directly relate to current measurements of particles at San Nicholas Island.

E. 22 OCTOBER 1984 CASE

The sequence of images on 22 October 1984 is the most intriguing of the period under study. A significant break in the prevailing northwesterly flow occurs from San Nicholas Island shoreward. A weak northeasterly flow is sustained from 1600 to 2300 GMT. Morning imagery from NOAA-6 (see Fig. 4.14) shows an extensive plume of low ratio values extending seaward from southern California metropolitan areas (A). A substantial low-ratio feature is seen to the southeast of San Nicholas Island (B). Ratio values range from highs of 1.84 over the open ocean to lows of 1.48 in the nearshore plume. The ratio value in the vicinity of San Nicholas Island is 1.68; San Nicholas Island lies just outside the influence of the large low-ratio feature (B) previously noted. The optical depth ratio from the sun photometer measurements at San Nicholas Island is 1.76.

Rawinsonde data recorded approximately three hours after image time (Fig. 4.15) indicates a fairly moist boundary layer, with a weak subsidence inversion near 800 - 700 mb. A later sounding (Fig. 4.16), recorded approximately two hours prior to NOAA-7 imagery, indicates a slight increase in moisture in the boundary layer, but otherwise little

change. A sounding obtained over land at Vandenberg Air Force Base, California at 1115 GMT shows a strong low-level inversion at 950 mb (Figure 4.17). In the absence of convective processes, aerosols generated within the boundary layer will tend to be trapped below the inversion.

In NOAA-7 imagery recorded in the afternoon (Fig. 4.18), the dark offshore feature (B) has moved west-southwestward in response to offshore flow. Increased streaking of the feature, in comparison to the NOAA-6 morning imagery, suggests that it is beginning to lose coherence. The maximum ratio value recorded by NOAA-7 is 1.68, and is lower than the morning NOAA-6 maximum. The minimum value within the plume to the west of the Los Angeles metropolitan area (A) is again 1.48. This sensor-to-sensor correlation indicates the continuity of this feature since the morning NOAA-6 pass.

Figs. 4.19 and 4.20 show the change in particle concentrations measured at San Nicholas Island between the NOAA-6 and NOAA-7 passes. Hourly concentration values (not presented) show small fluctuations throughout the day, which are believed to correlate to the passage of the northern tip of the low-ratio feature across San Nicholas Island.

TABLE III

Measurements of Aerosol Optical Thickness,
22 October 1984

Local Time	t: 0.64um	t: 0.88um	t(.64)/t(.88)
0827	.088	.050	1.76
0836	.071	.032	2.21
0845	.074	.041	1.80
0857	.077	.051	1.51
0947	.098	.060	1.63
1054	.119	.075	1.59
1110	.112	.071	1.58
1116	.101	.067	1.51
1124	.096	.064	1.50
1244	.102	.073	1.40
1252	.113	.093	1.22
1259	.120	.102	1.18
1318	.112	.096	1.17

A series of measurements of total atmospheric aerosol optical depth, τ, as measured by a sun photometer at San Nicholas Island, is presented in Table III. The measurements were recorded for wavelengths of 0.64 and 0.88 microns, corresponding to the spectral bands of the AVHRR channels 1 and 2. Rapid fluctuations of the readings, and the substantial decrease in the ratios of the two values near the noon hour are also believed to relate to the passage of the low-ratio feature. The net change in particulate concentrations noted during the day, as seen by comparing Figs. 4.19 and 4.20, is a decrease in supermicron particles and a slight increase in submicron particles. The ratio values in the immediate vicinity of San Nicholas Island as indicated by NOAA-7 in the afternoon are near 1.60. There are rapid spatial fluctuations in the ratio values near San Nicholas Island apparent in both the NOAA-6 and NOAA-7 imagery, which make it difficult to relate the average values of aerosol concentrations measured by the particle counters to averaged ratio values observed around San Nicholas Island. Nevertheless, there are no large changes in values of either the particulate concentrations or the ratio values. The low-ratio values attained by the sun photometer optical depth ratios at mid day follow the relative progression of low ratios as seen in the imagery near San Nicholas Island. Along the coast, the area of lowest ratio, which is south of the Long Beach area in the morning, is seen to have moved westward beyond the extent of the Palos Verdes Peninsula by afternoon. This represents direct evidence of seaward advection of urban particles.

F. 23 OCTOBER 1984 CASE

On the 23rd of October 1984, weak offshore winds were again maintained throughout the mid-day period, similar to conditions encountered on the 22nd. Afternoon imagery from NOAA-7, Fig. 4.21, again shows a prominent plume of very low

(to a minimum of 1.18) ratios extending seaward from the Los Angeles and Orange County areas (A), with lesser dark plumes to the north in the vicinity of Ventura and Oxnard (B). The striated area in the lower portion of the image, to the south of San Nicholas Island (C), is believed to represent the remnants of the offshore feature discussed on the 22nd of October. High ratio values of from 1.65 to 1.74 are present to the west of San Nicholas Island. This high-ratio area indicates a region of increased concentration of submicron particles, with respect to the rest of the image. If it is assumed that the low-ratio plumes near the coast represent the presence of urban and terrestrial particles in the boundary layer which have grown due to humidity effects, then the high-ratio areas over the open ocean represent areas of decreased contamination in the boundary layer.

Rawinsonde data taken at 1700 GMT, Fig. 4.22, show a moist surface layer with dry conditions aloft. A later sounding at 2120 GMT, Fig. 4.23, shows a marked drop in moisture. This sounding is the driest encountered in the period under study. Early morning particle concentrations, Fig. 4.24, show similar values to those recorded on the evening of the 22nd (Fig. 4.20). However, by three hours later there has been a precipitous drop in the concentrations of supermicron particles; see Fig. 4.25. By late afternoon, near image time, the supermicron particles have again appeared, but in concentrations much less than their morning values (see Fig. 4.26). Submicron particles evidence a slow, steady net rise throughout the day. Supermicron particle behavior in response to the rapid drying of the lower troposphere, as evidenced in the soundings, is as expected. No image data exists in the period of supermicron particle minimums with which to examine associated ratio values. The ratio values in the vicinity of San Nicholas Island average near 1.60, which is

a similar value to that recorded on the previous afternoon. By comparison, the ratio of optical depth values optained from the sun photometer is 1.37. Examination of Fig. 4.21 shows that San Nicholas Island lies at a boundary of high and low ratio values. The higher values that impinge on San Nicholas Island are consistent with the measured relationship between sub- and supermicron particles, which itself is consistent with the observed decrease in atmospheric moisture levels.

G. 24 OCTOBER 1984 CASE

On 24 October 1984, north-northwesterly flow was again established in the southern California coastal area, and no evidence of offshore transport is seen (Fig. 4.27). Ratio values from NOAA-7 imagery are lower than those of the previous two days, an expected response to a predominately marine environment. Values range from a low of 1.32 to a high of 1.65; values near San Nicholas Island average 1.37. The ratio of optical depths measured by the sun photometer at San Nicholas Island is 1.20.

Sounding data taken at 2058 GMT, two hours prior to image time, show a fairly moist surface layer with moderately dry conditions aloft (Fig. 4.28). Figs. 4.29 and 4.30 show a sharp decline in supermicron particles during the day. The submicron particles fluctuate during the day, but end (at image time) with concentrations similar to their morning values, which were less than those recorded during the very dry conditions of the previous afternoon. This decrease in submicron particle levels from those of the 23rd supports the lower ratios in the imagery of the 24th.

H. 25 OCTOBER 1984 CASE

On the 25th of October 1984, winds were calm throughout the day with a light offshore component. Morning imagery from NOAA-6 (Fig. 4.31) shows some slight indication of

offshore particle transport as evidenced by small low-ratio plumes along the coast (A). Note however that the apparent low-ratio area to the northeast of Santa Catalina Island was investigated in the AVHRR channel 4 infrared imagery and determined to be light cirrus contamination. A major portion of the image is in fact obscured by cirrus, including San Nicholas Island, which precludes direct comparisons between image ratios and particle concentrations. With the exception of the small low-ratio regions along the coast, where ratios down to 1.39 are encountered, minimum and maximum values are well dispersed throughout the image, ranging from 1.48 to 1.62.

The concentration of submicron particles increases throughout the day, while that of supermicron particles remains relatively constant (Figs. 4.32 and 4.33). Although the ratio values at San Nicholas Island are not available, the moderate (as compared to previous days) range of values observed elsewhere in the imagery is consistent with the low concentrations of submicron particles measured near image time. The 2120 GMT sounding, Fig. 4.34, taken nearly four and one half hours after image time, shows relatively dry conditions at the surface.

I. DISCUSSION OF RESULTS

The particle concentrations measured at the surface respond in an expected, predictable manner to changes in relative humidity. Specifically, drying implies an increase in the relative number of submicron particles, as available aerosols give up water through evaporation, and this is borne out by experimental results. Similarly, an increase in available moisture is expected to stimulate the growth of particles. This process is evidenced by the decrease in concentration of submicron particles on 19 October 1984.

No well-defined air mass change, such as that expected during a sharp cold frontal passage, was experienced during

the examined timeframe. Thus the contrasts in levels of particulate matter in the lower- and mid- troposphere expected between major air masses could not be examined. A weak frontal event occurring immediately prior to the experiment period may have possibly affected data acquired on the 17th of October 1984. Certainly, the relatively lower concentrations of submicron particles measured on that day, as compared to dry days of the experiment, exhibit an expected post-frontal pattern. Low ratio values obtained from NOAA-7 on the 17th support a reduced concentration of submicron particles. However, the image data must be viewed with caution in light of possible sunglint contamination of these values.

However, more subtle changes in air mass characteristics were noted during the experiment. The moisture content of the lower troposphere showed some notable variations, and particle concentrations and ratio values were observed to respond to these changes in moisture levels.

To investigate this correspondence, total aerosol optical depth measured by a sun photometer at San Nicholas Island was compared with ratio values. The optical depth value for wavelengths of .64 and .88 microns were ratioed, and the results compared to the AVHRR channel 1 and channel 2 ratios observed in the vicinity of San Nicholas Island. Variations in satellite-measured ratio values should relate directly to variations in photometer- measured optical depth ratios. A relationship was therefore sought between the two ratios. The results are presented in Fig. 4.35, and show good agreement, with a correlation coefficient of 0.72, and significance level of greater than 95 percent. Fig. 4.35 indicates a slight high bias in the channel 1 / channel 2 ratios as compared to the photometer data. This bias is believed to result from the fact that the Rayleigh component of optical depth has been removed from the photometer data.

This was not done for the Rayleigh contribution to radiance in the imagery. The effect of Rayleigh scattering is to slightly increase the radiance levels in the red spectrum. The red / near-infrared ratio values will therefore be slightly higher when imagery is not corrected for Rayleigh scattering. Good correlation of the uncorrected ratio values to the sun photometer data supports the simplified procedure utilized in this study.

Examination of the wind fields and ratio values show that, for the period of this study, San Nicholas Island tended to lie at or near a transition point for surface and near-surface processes. To the west of San Nicholas Island, a very consistent northwesterly flow regime was maintained, indicative of predominately marine processes in that region. To the east, conditions were variable, with predominately onshore flow at night, but with offshore flow of varying intensity and extent sometimes encountered during mid-day. A suggestion of this line of demarcation (of lower tropospheric processes) extending roughly southeastward from Point Concepcion is apparent in several of the ratio image patterns presented, specifically Figs. 4.2, 4.5, 4.14, 4.18, 4.21 and 4.27. Aerosol events occurring within the Southern California Bight, as evidenced by the low-ratio plume features during periods of offshore flow, did not, generally, impact on San Nicholas Island, and when they did, did so only peripherally. Thus, data acquired at or over San Nicholas Island cannot be held as representative of all processes and events depicted in the imagery.

Aerosol distributive processes vary temporally and spatially. The distribution and transport of atmospheric aerosols in and above the marine boundary layer cannot be explained by a single mechanism. Rather, different local and regional models must be constructed. Through the selection of an appropriate model for the origin and transport of

aerosols, the multi-channel ratio technique may be applied to infer vertical distributions. For instance, in the period of September and October 1982 investigated by Durkee (1986), terrestrial aerosols were convectively transported above the boundary layer, where, under the influence of reduced atmospheric moisture content, they remained relatively small. The horizontal transport of these particles seaward above the marine boundary layer was shown by an increase in ratio values for red and near-infrared wavelengths. In the 1984 data, for the same region at the same season, a different transport mechanism was in effect. Terrestrial aerosols, apparently of urban origin, tended to remain within the boundary layer, and to grow through accretion of water vapor. Thus, the boundary layer was characterized by an increase in concentration of supermicron particles, and the transport of the urban particles seaward was evidenced by a decrease in red to near-infrared ratios. Figure 4.36 illustrates a proposed model for this behavior. Urban aerosols generated within the boundary layer are trapped below a capping inversion. Turbulent mixing and transport above the boundary layer is absent, due to a lack of radiative heating over land. The urban particles are advected seaward by offshore winds within the boundary layer.

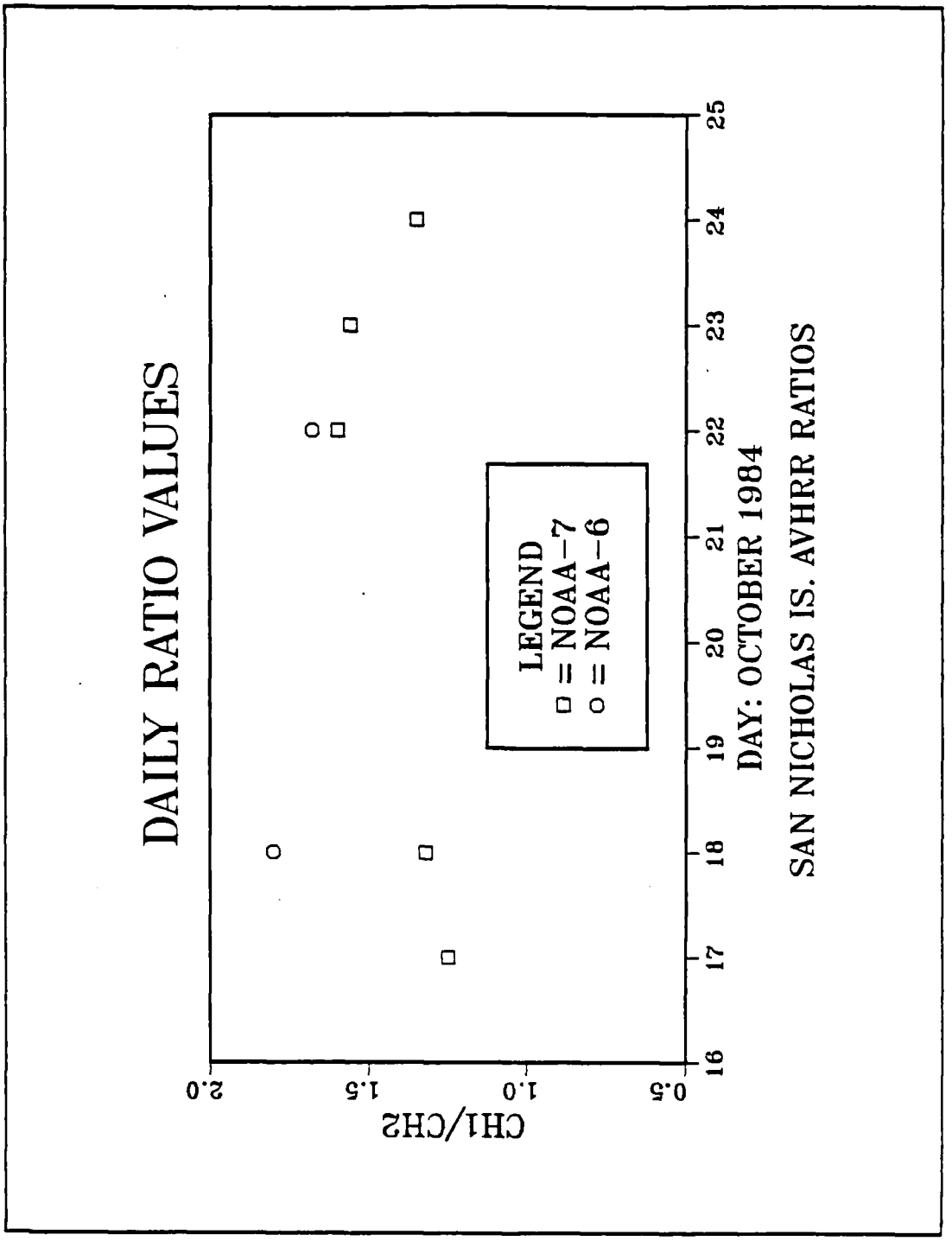

Fig. 4.1 Time series of NOAA-6 and NOAA-7 AVHRR channel 1 and channel 2 ratio values.

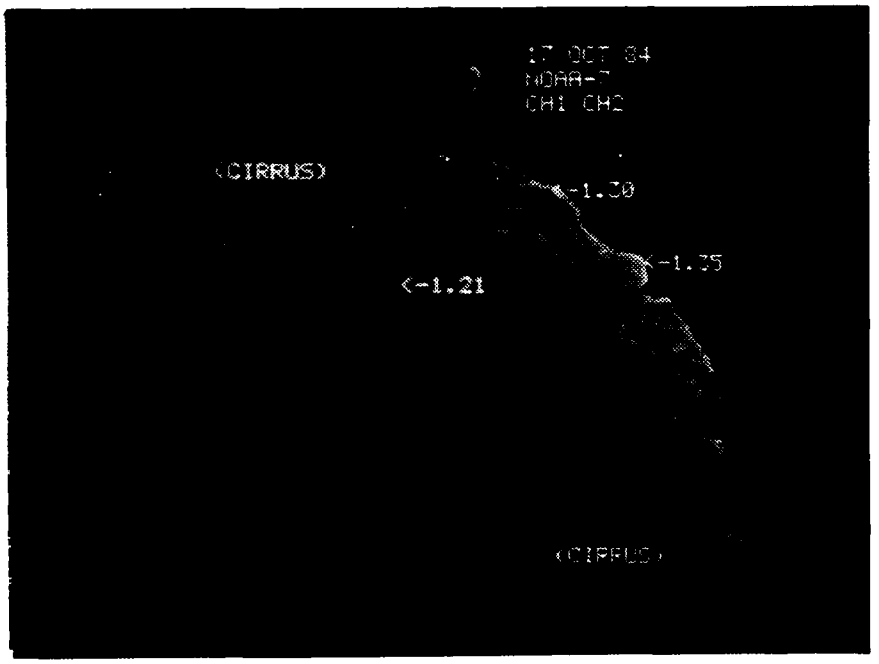

Fig. 4.2 NOAA-7 Channel 1 / Channel 2 ratio image, 2247 GMT, 17 October 1984.

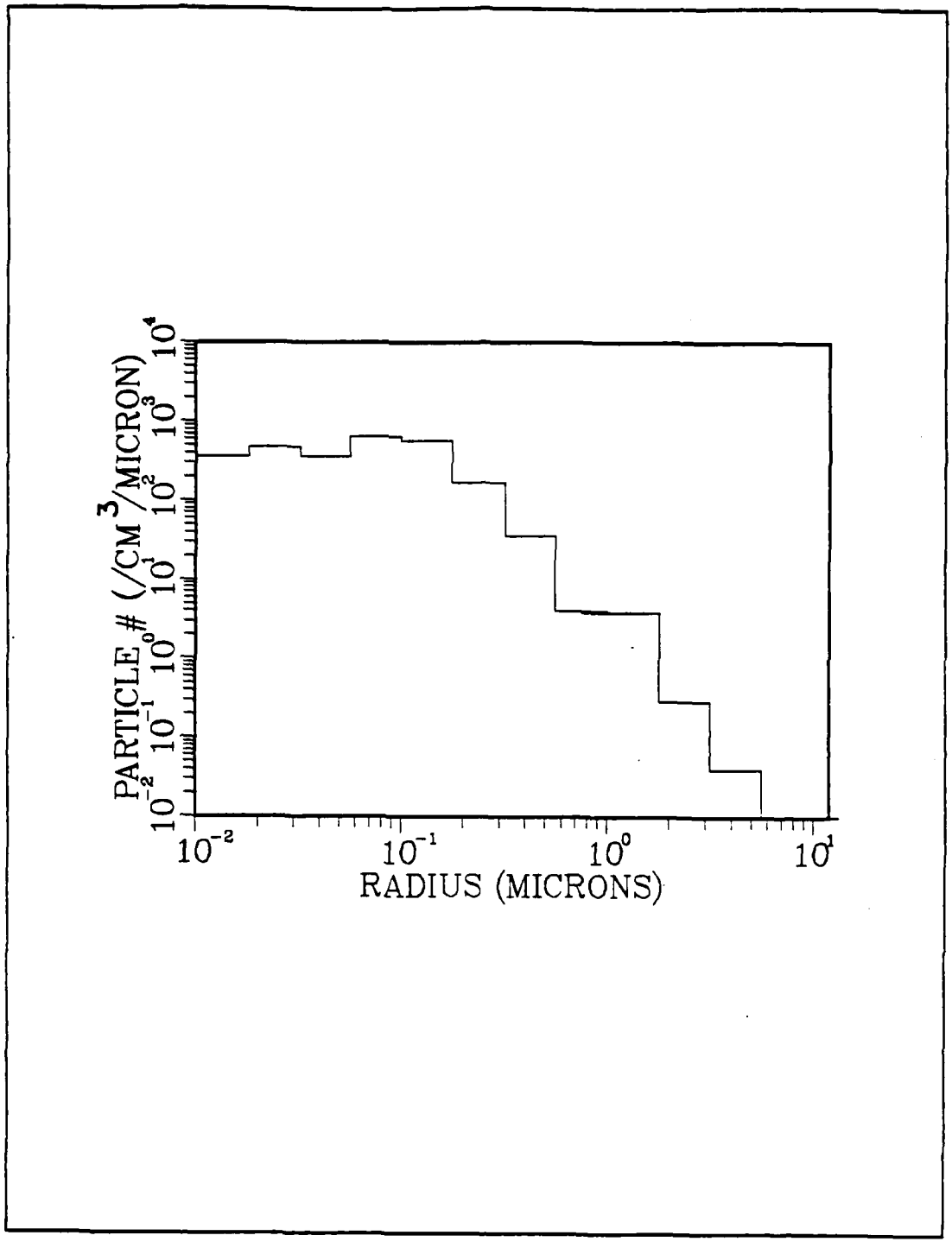

Fig. 4.3 Particle concentrations, 2300 GMT, 17 October 1984.

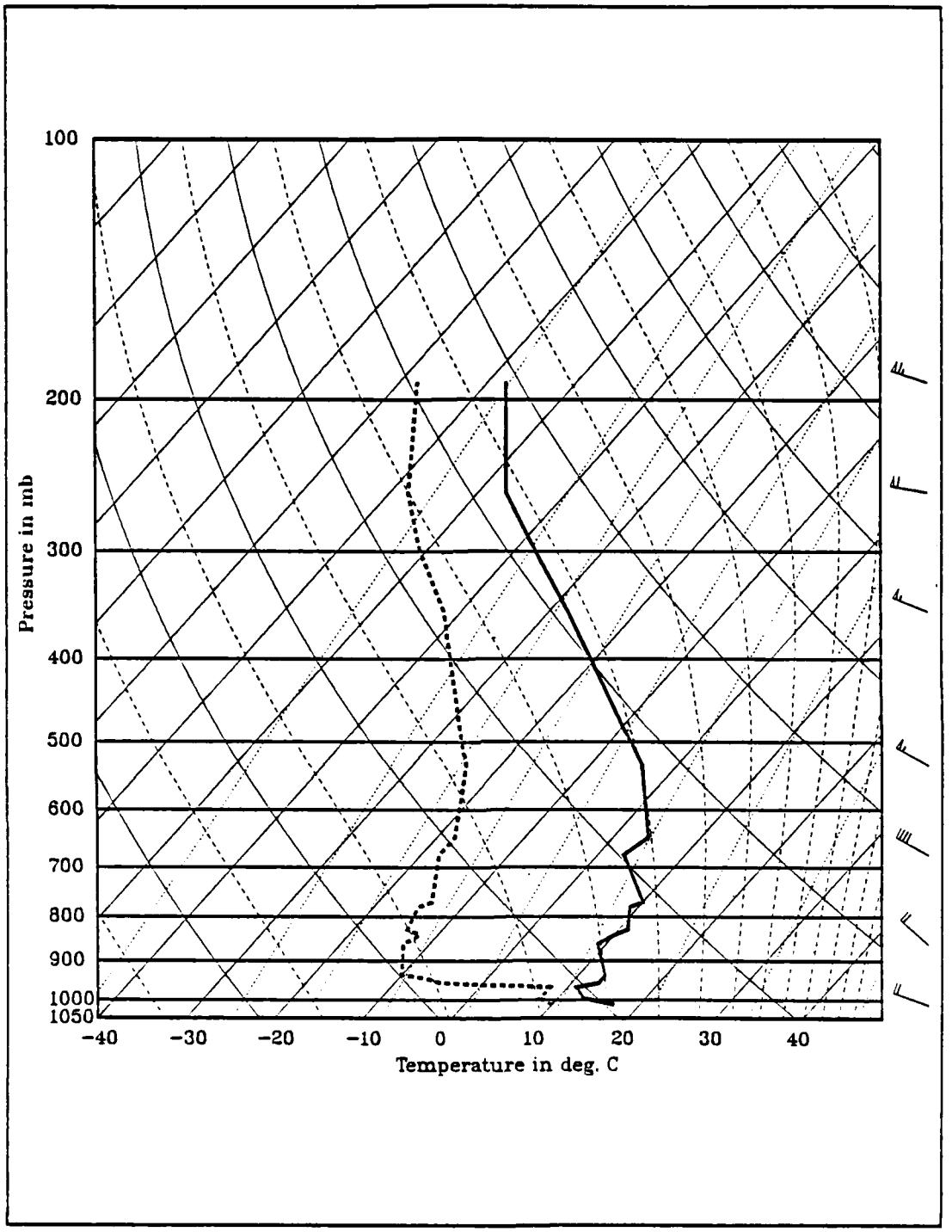

Fig. 4.4 San Nicholas Island rawinsonde observation, 2051 GMT, 17 October 1984.

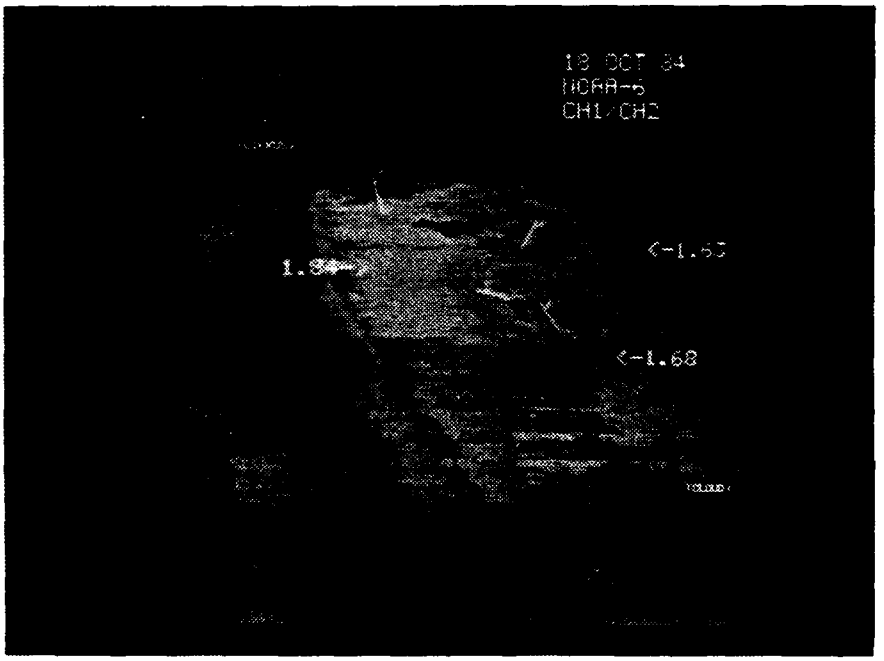

Fig. 4.5 NOAA-6 Channel 1 / Channel 2 ratio image, 1507 GMT, 18 October 1984.

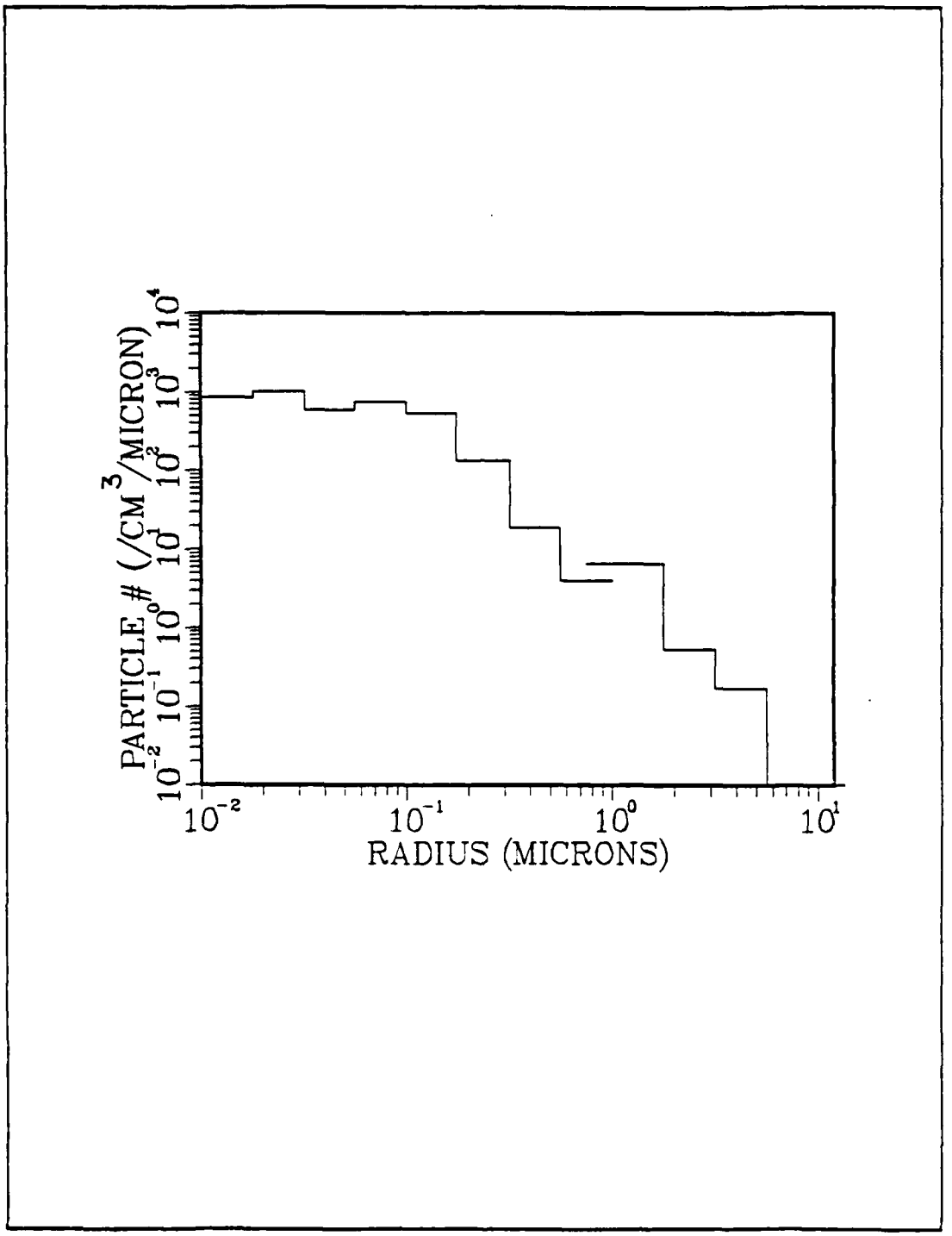

Fig. 4.6 Particle concentrations, 1500 GMT, 18 October 1984.

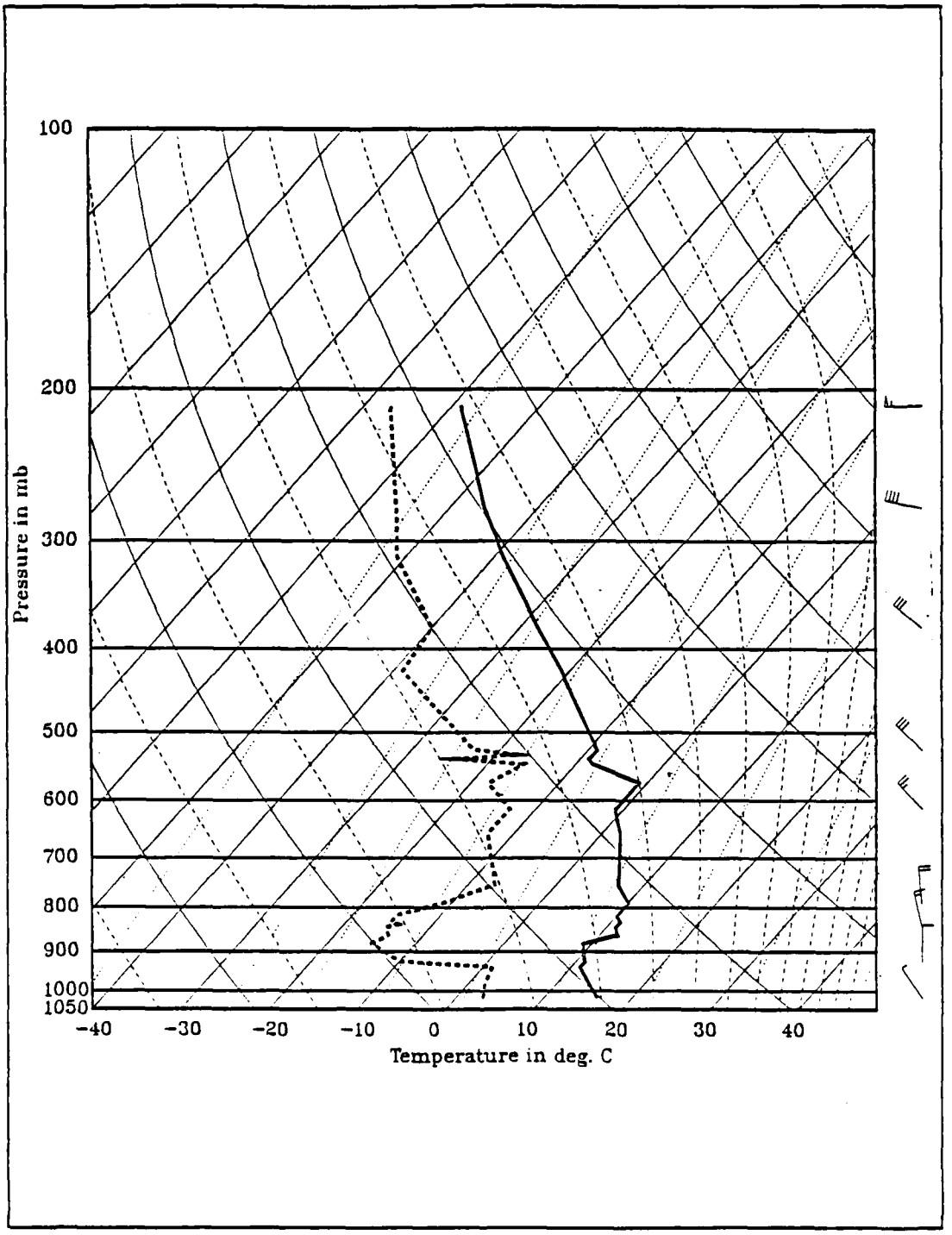

Fig. 4.7 San Nicholas Island rawinsonde observation, 2113 GMT, 18 October 1984.

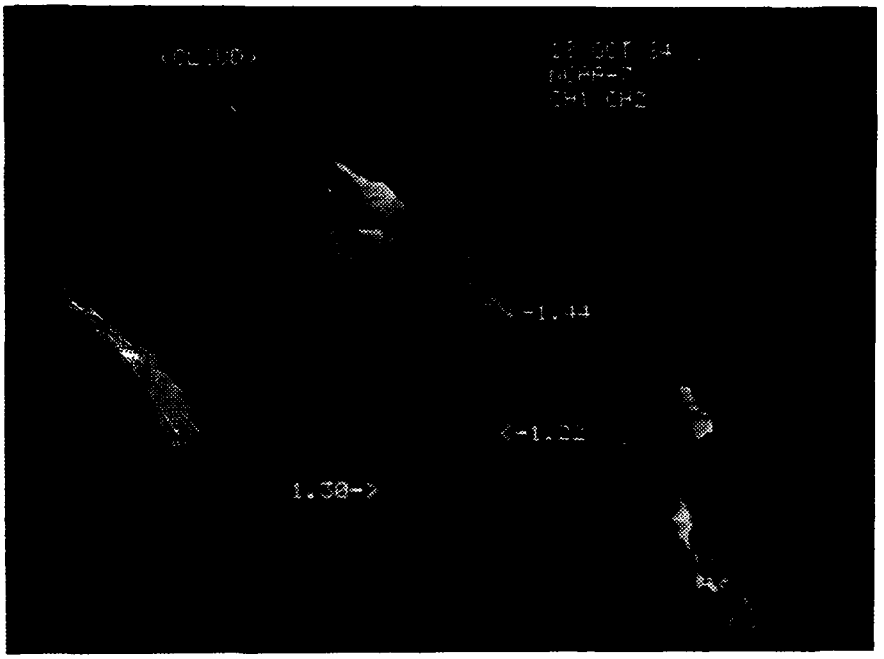

Fig. 4.8 NOAA-7 Channel 1 / Channel 2 ratio image, 2235 GMT, 18 October 1984.

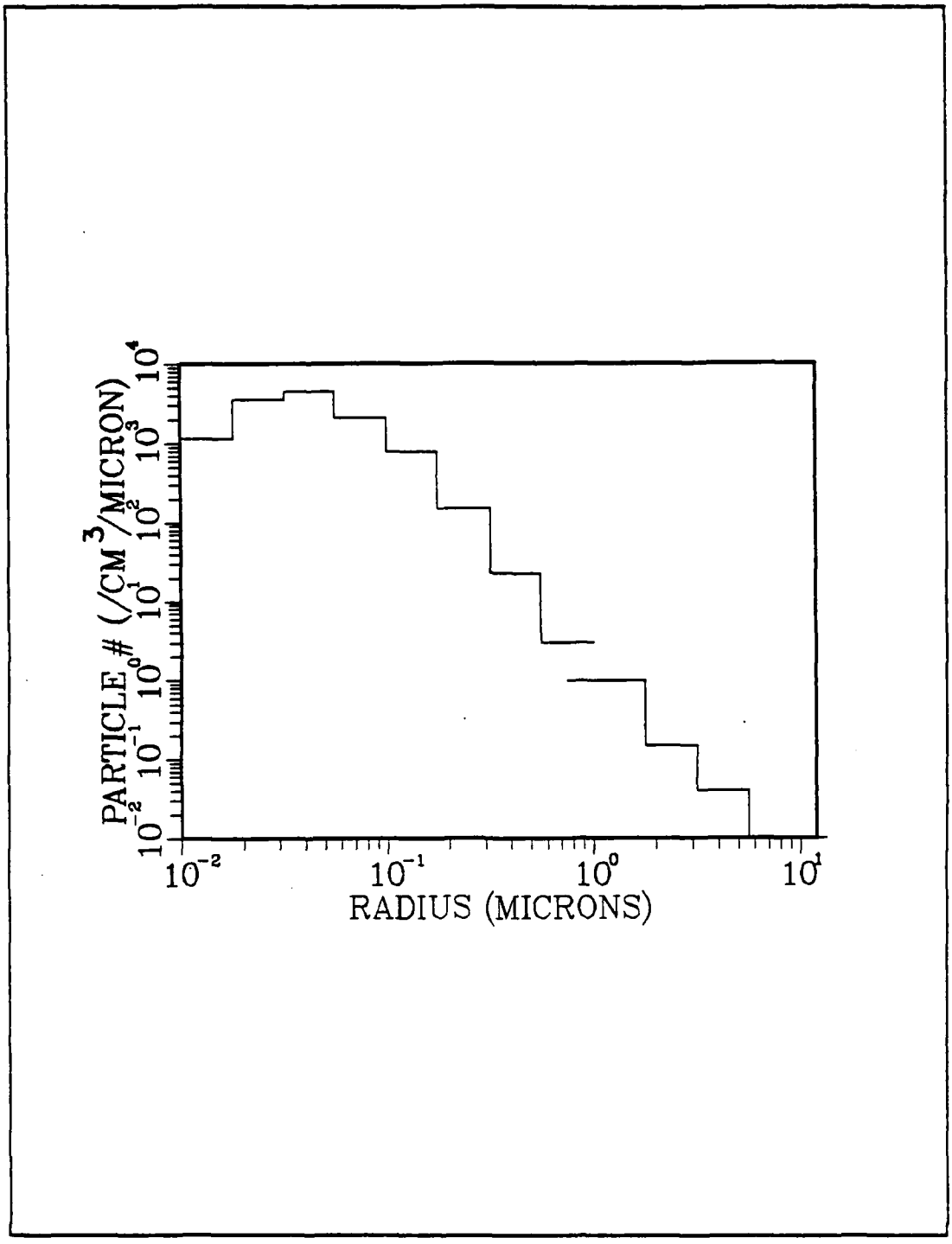

Fig. 4.9 Particle concentrations, 2300 GMT, 18 October 1984.

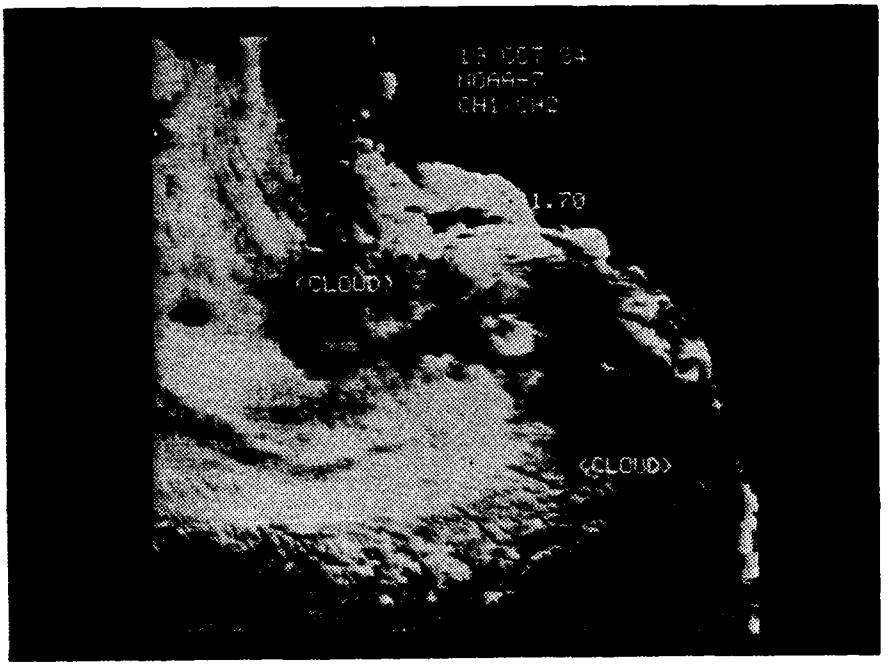

Fig. 4.10 NOAA-7 Channel 1 / Channel 2 ratio image, 2359 GMT, 19 October 1984.

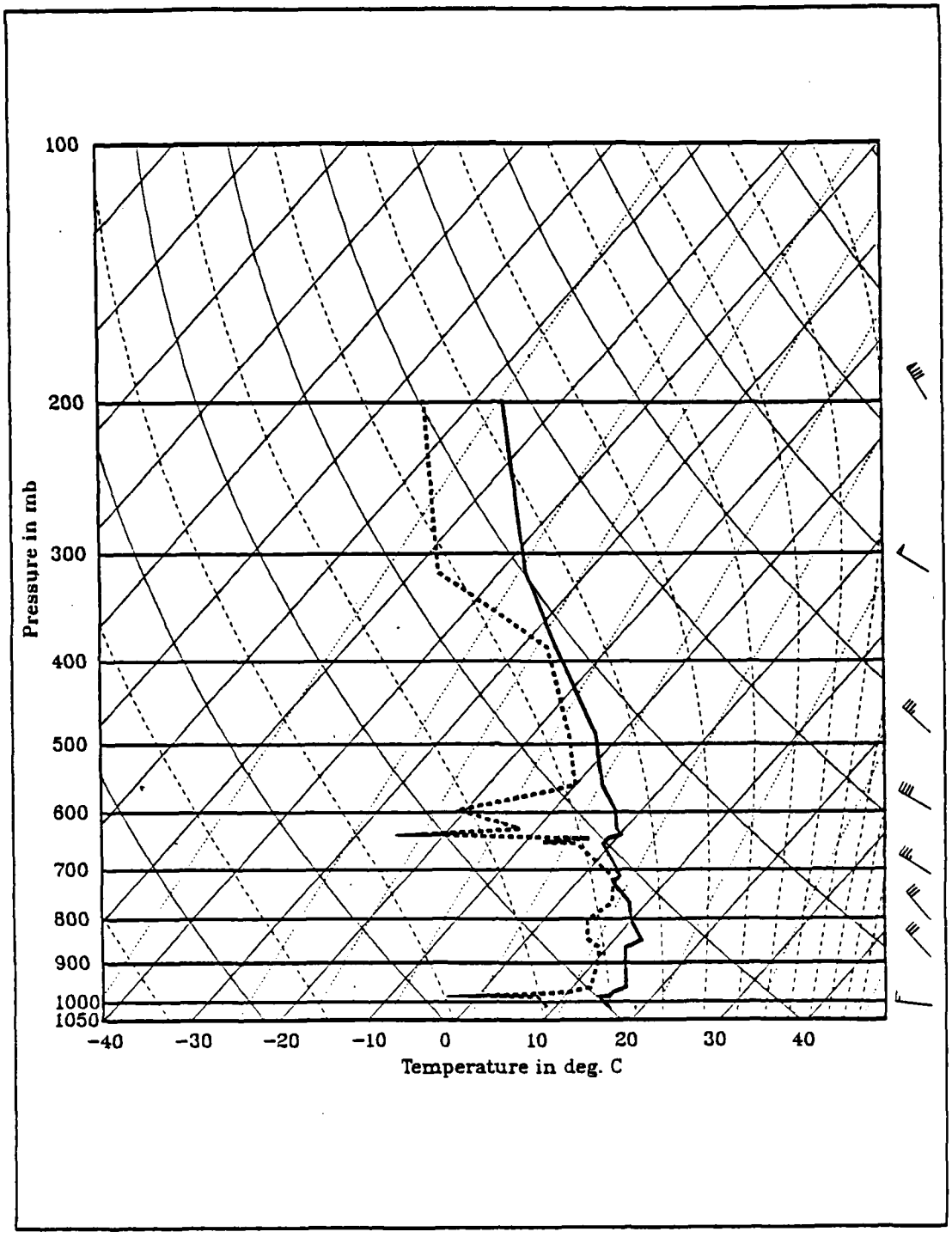

Fig. 4.11 San Nicholas Island rawinsonde observation, 1534 GMT, 19 October 1984.

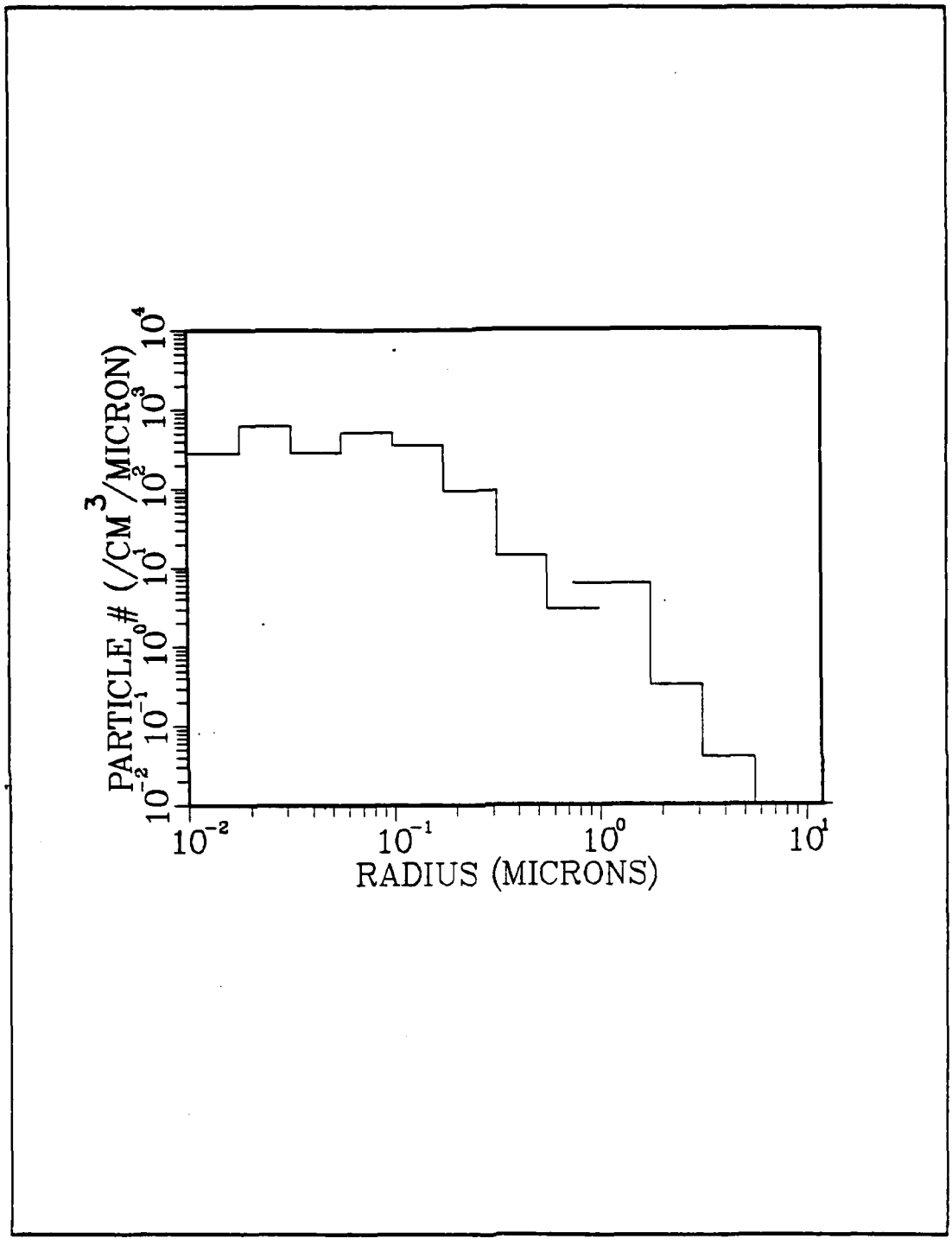

Fig. 4.12 Particle concentrations, 1500 GMT, 19 October 1984.

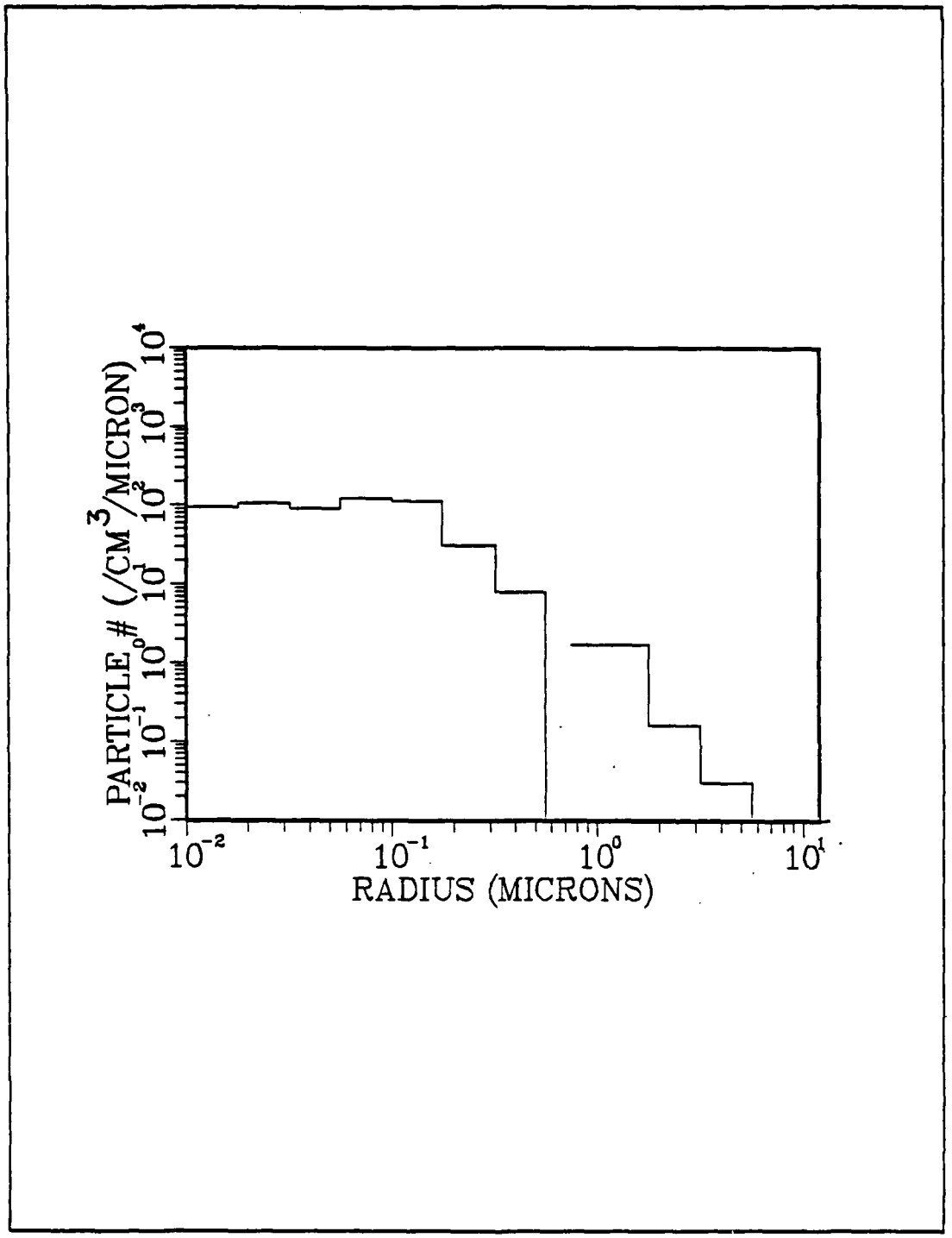

Fig. 4.13 Particle concentrations, 2400 GMT, 19 October 1984.

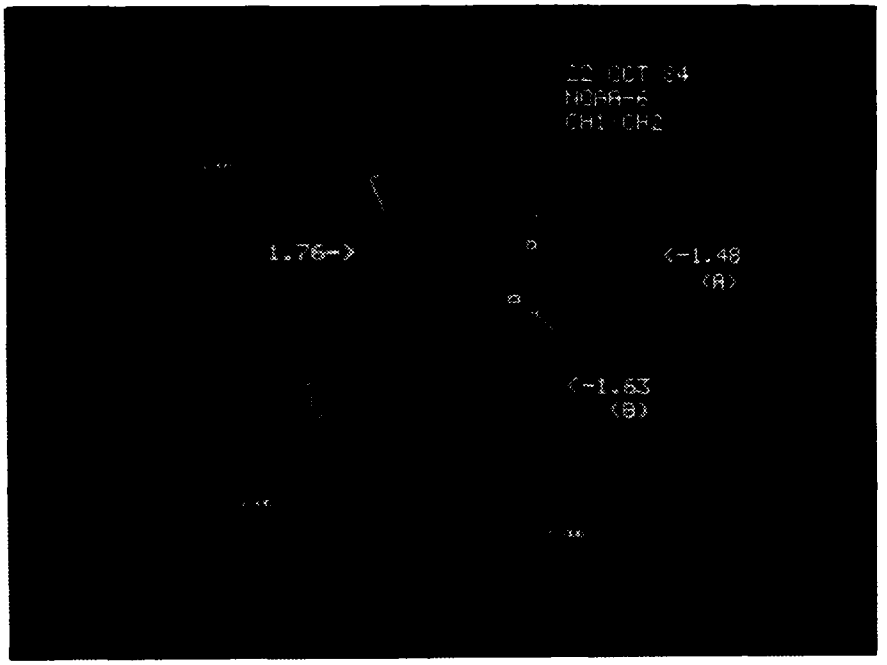

Fig. 4.14 NOAA-6 Channel 1 / Channel 2 ratio image, 1511 GMT, 22 October 1984.

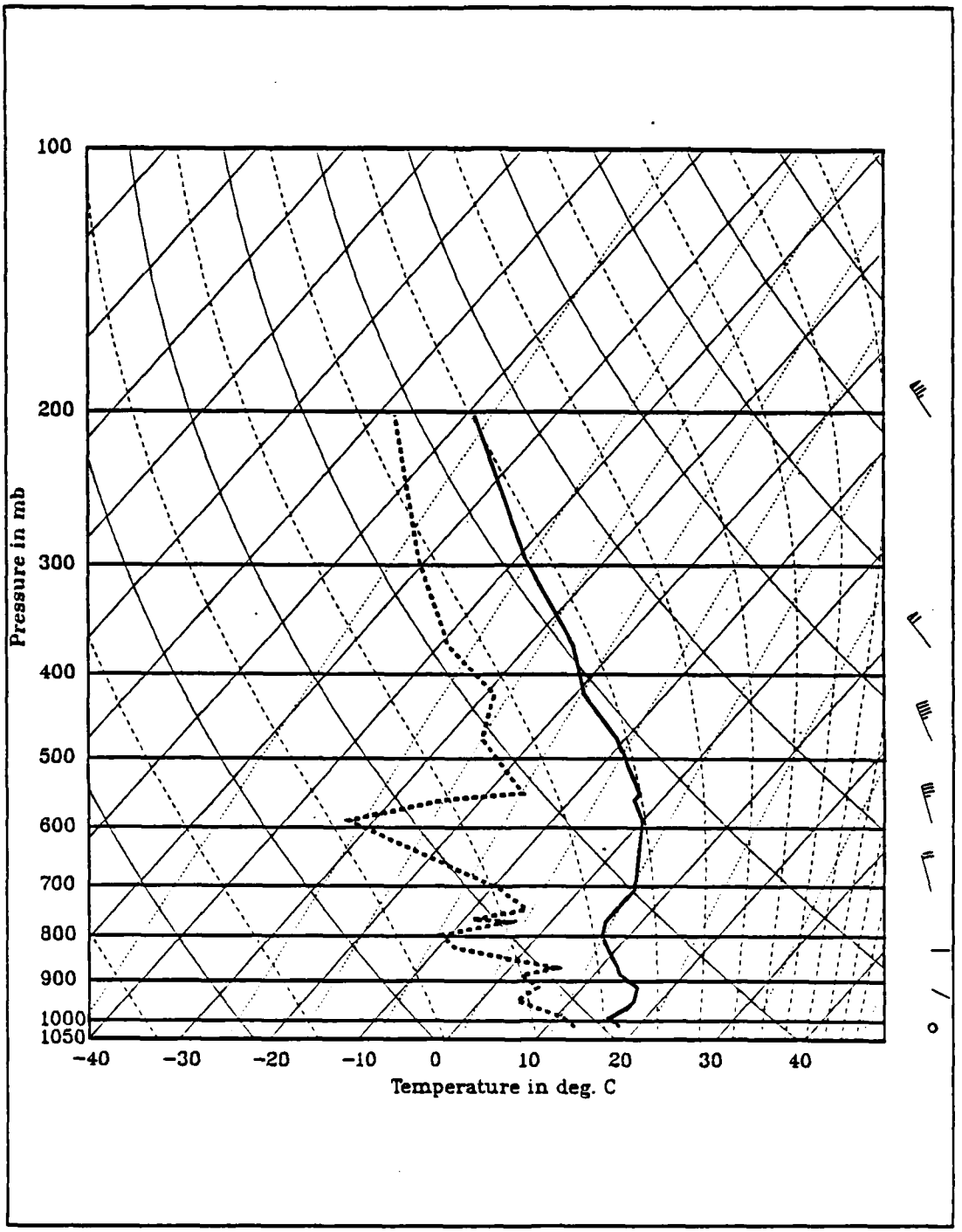

Fig. 4.15 San Nicholas Island rawinsonde observation, 1821 GMT, 22 October 1984.

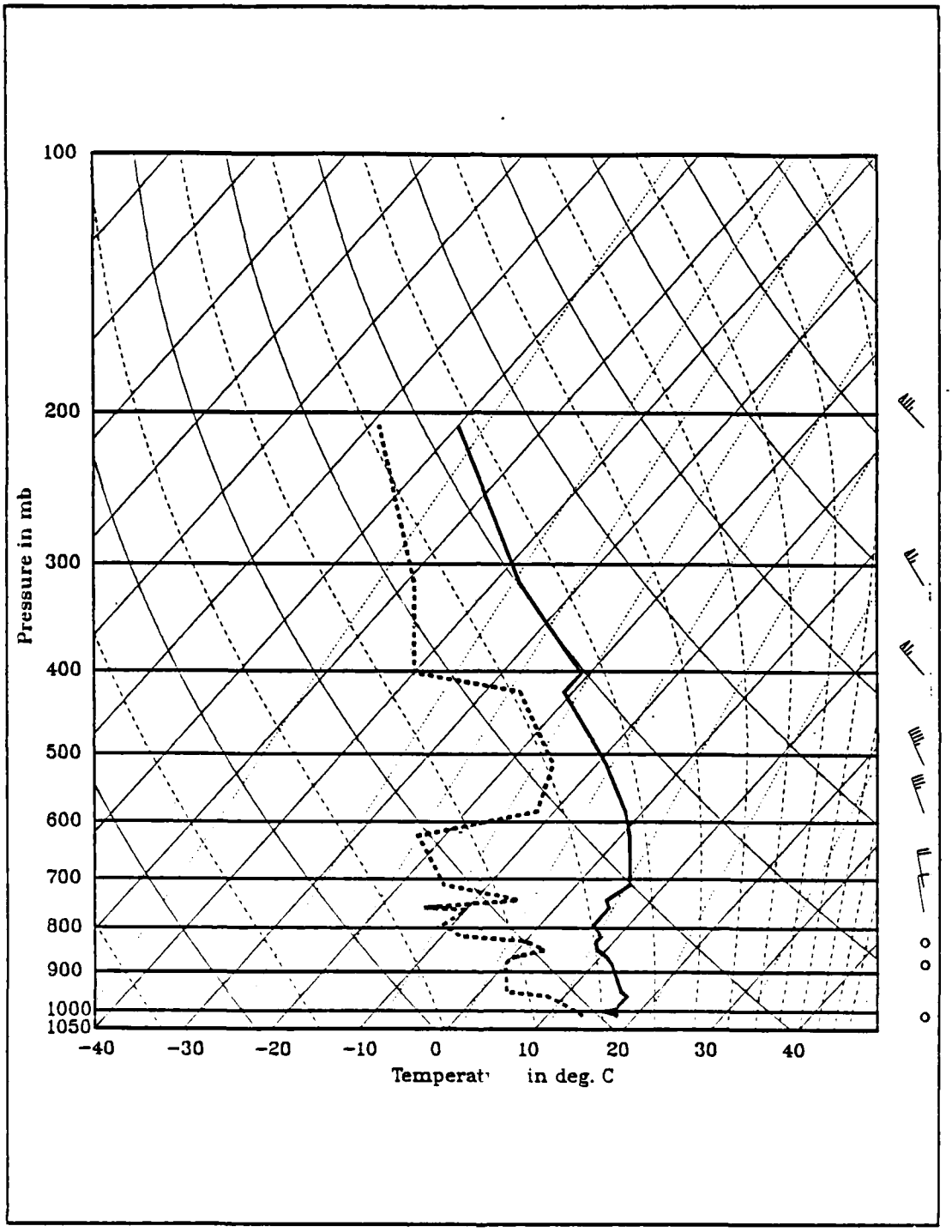

Fig. 4.16 San Nicholas Island rawinsonde observation, 2139 GMT, 22 October 1984.

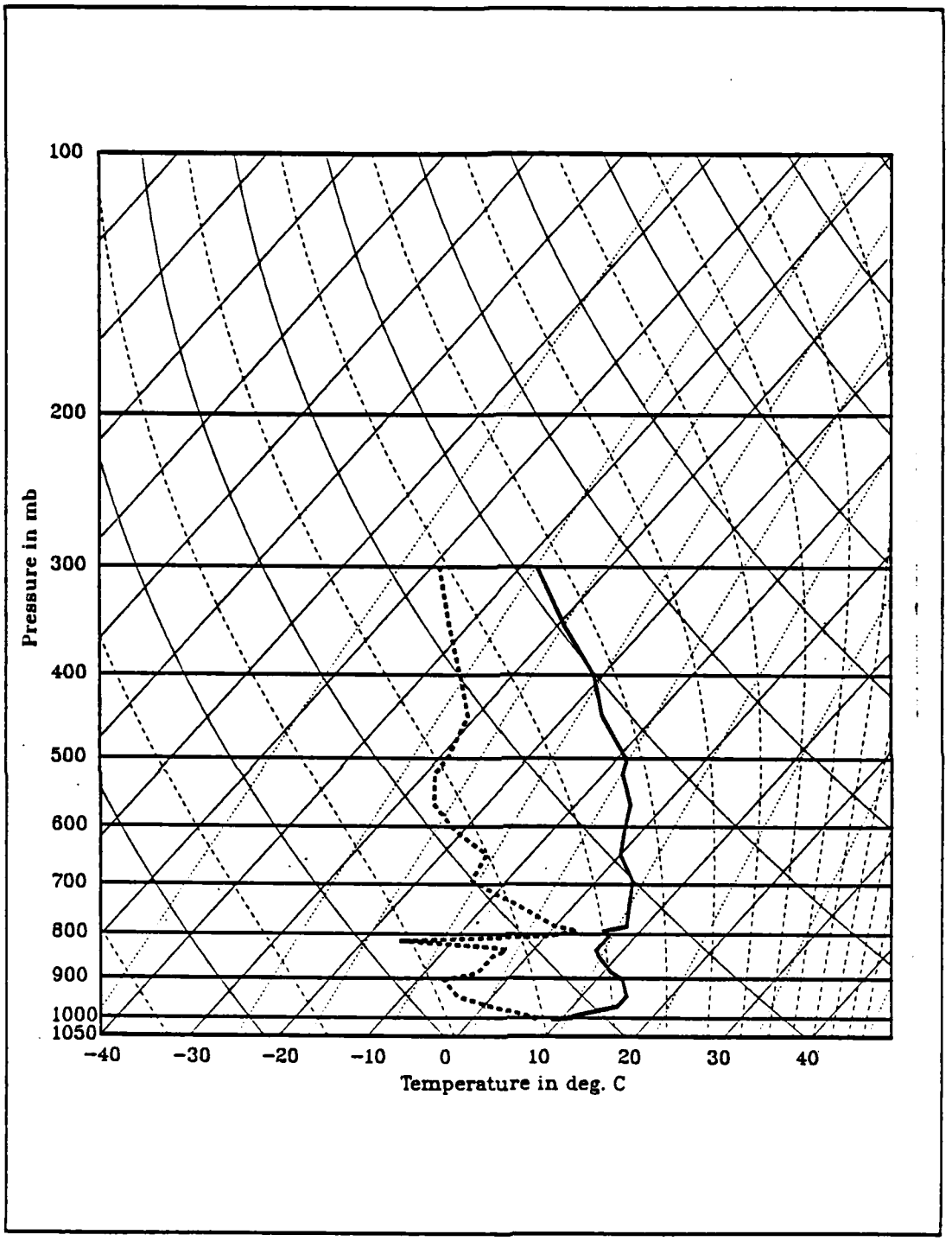

Fig. 4.17 Vandenberg AFB rawinsonde observation, 1115 GMT, 22 October 1984.

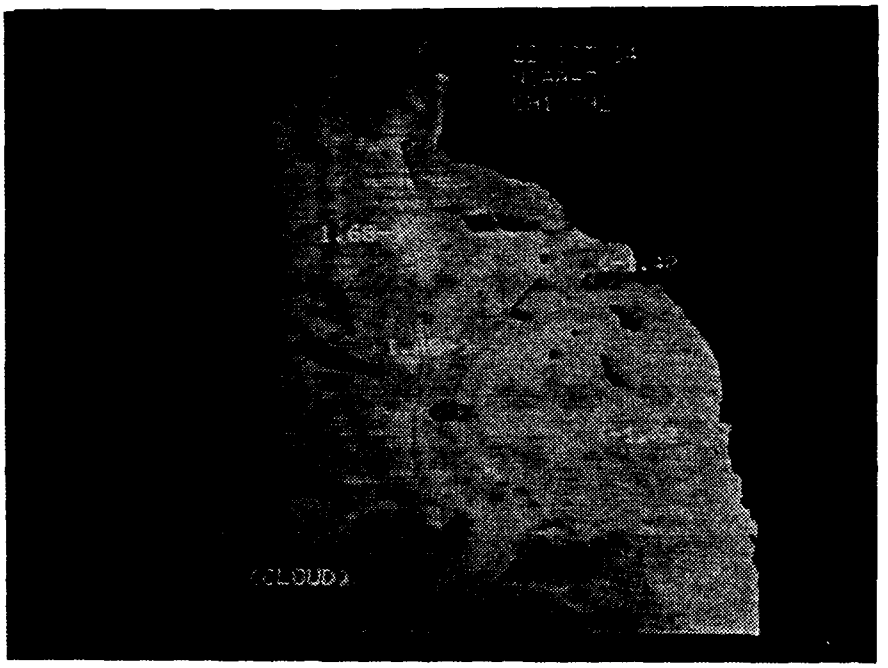

Fig. 4.18 NOAA-7 Channel 1 / Channel 2 ratio image, 2326 GMT, 22 October 1984.

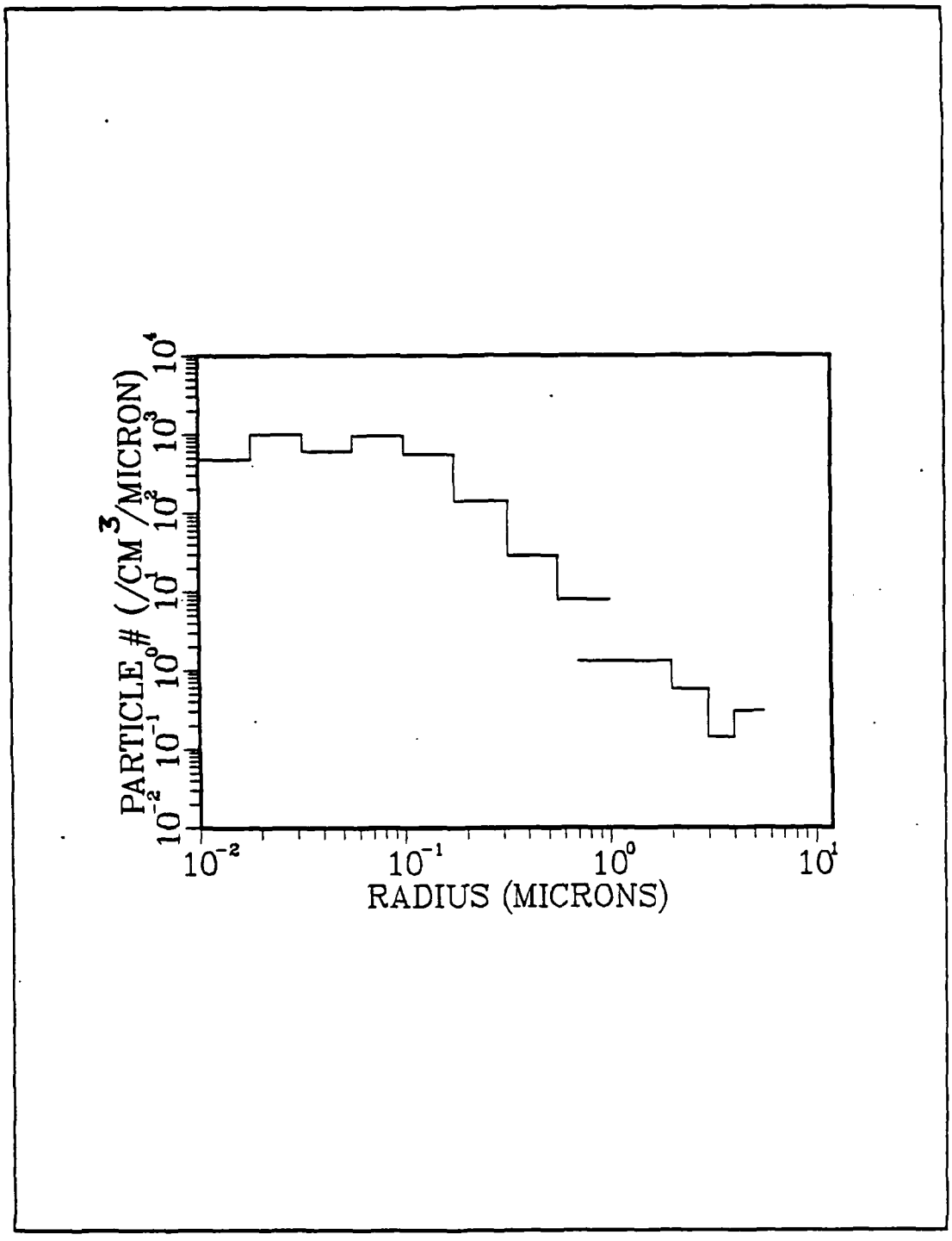

Fig. 4.19 Particle concentrations, 1500 GMT, 22 October 1984.

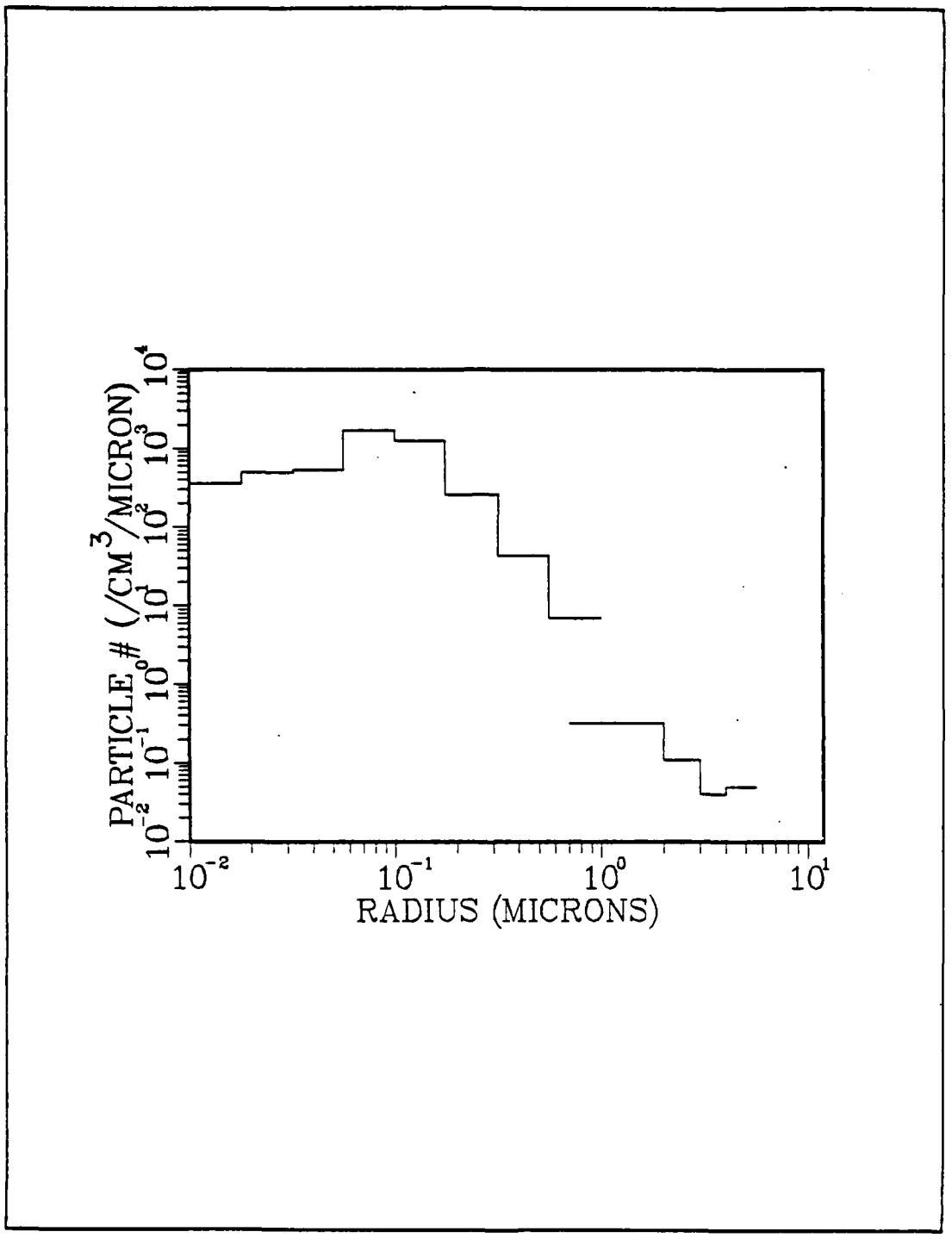

Fig. 4.20 Particle concentrations, 2400 GMT, 22 October 1984.

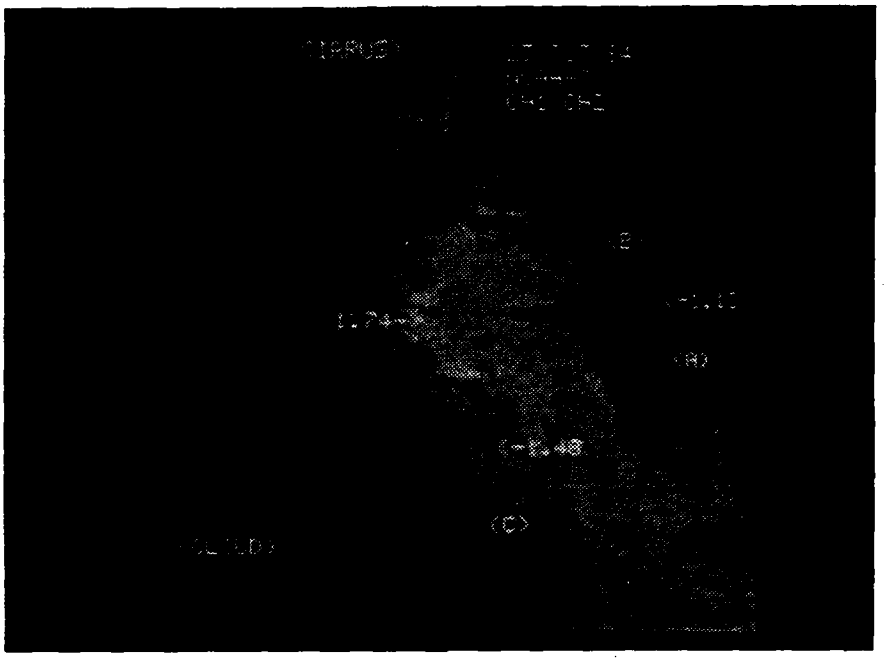

Fig. 4.21 NOAA-7 Channel 1 / Channel 2 ratio image, 2300 GMT, 23 October 1984.

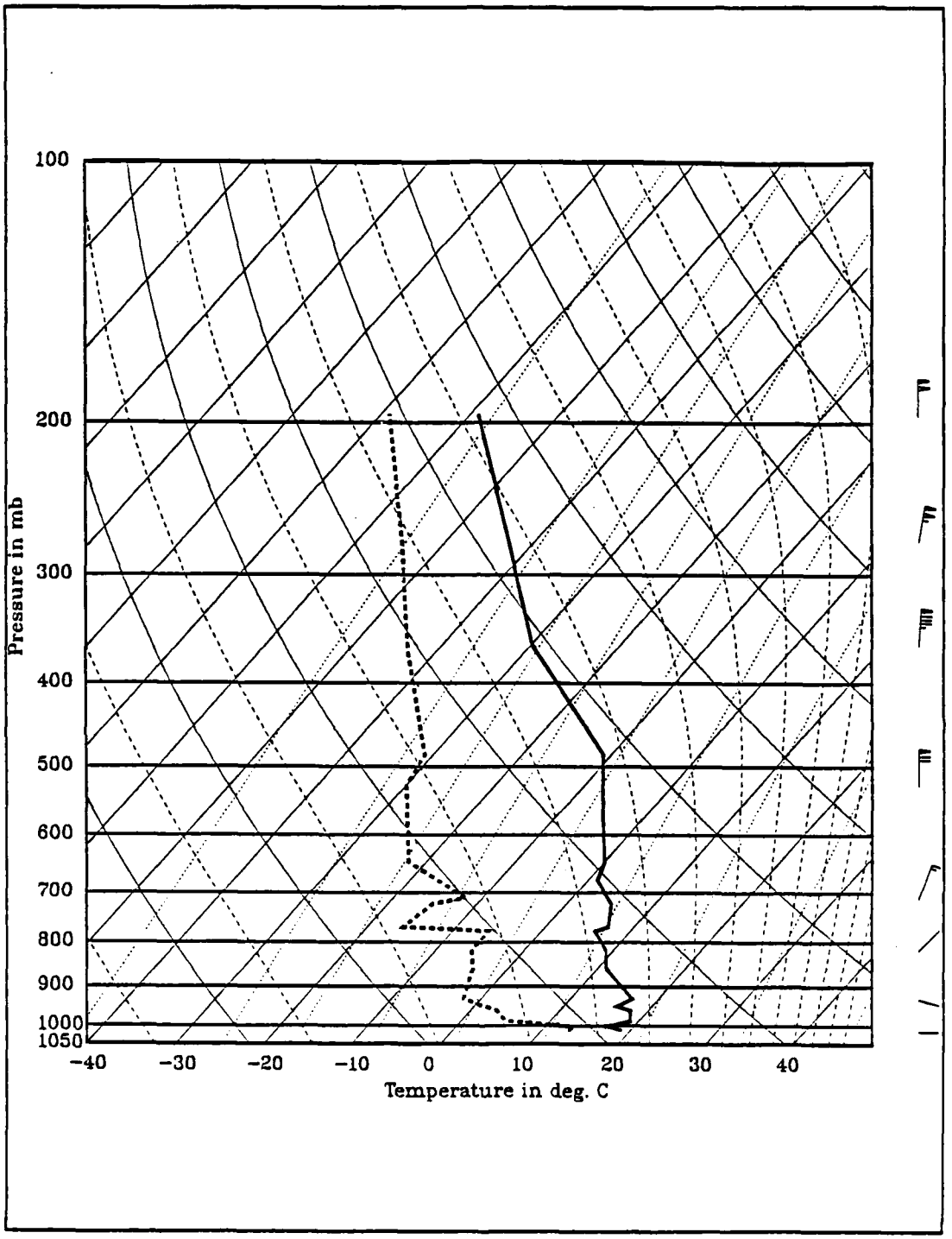

Fig. 4.22 San Nicholas Island rawinsonde observation, 1700 GMT, 23 October 1984.

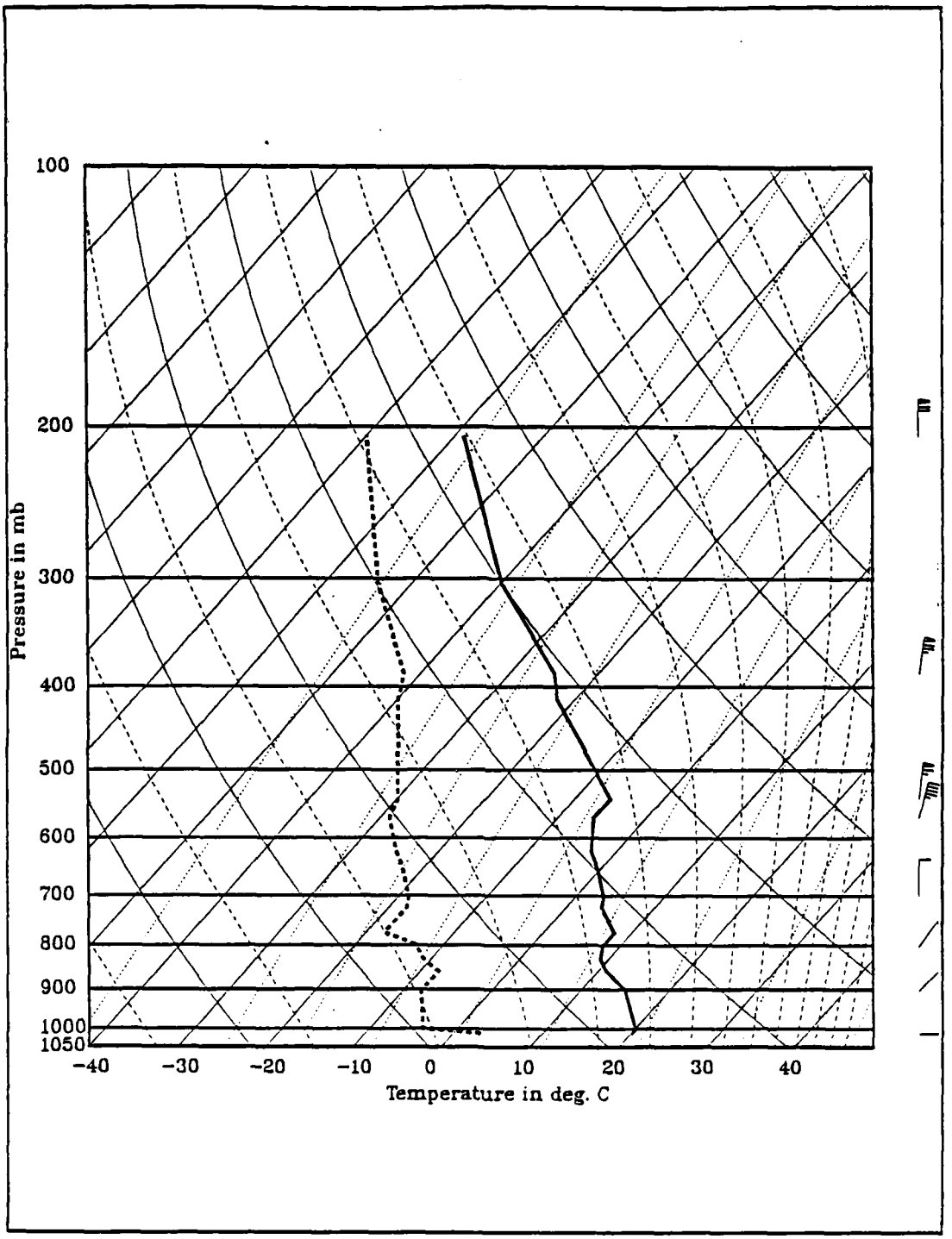

Fig. 4.23 San Nicholas Island rawinsonde observation, 2120 GMT, 23 October 1984.

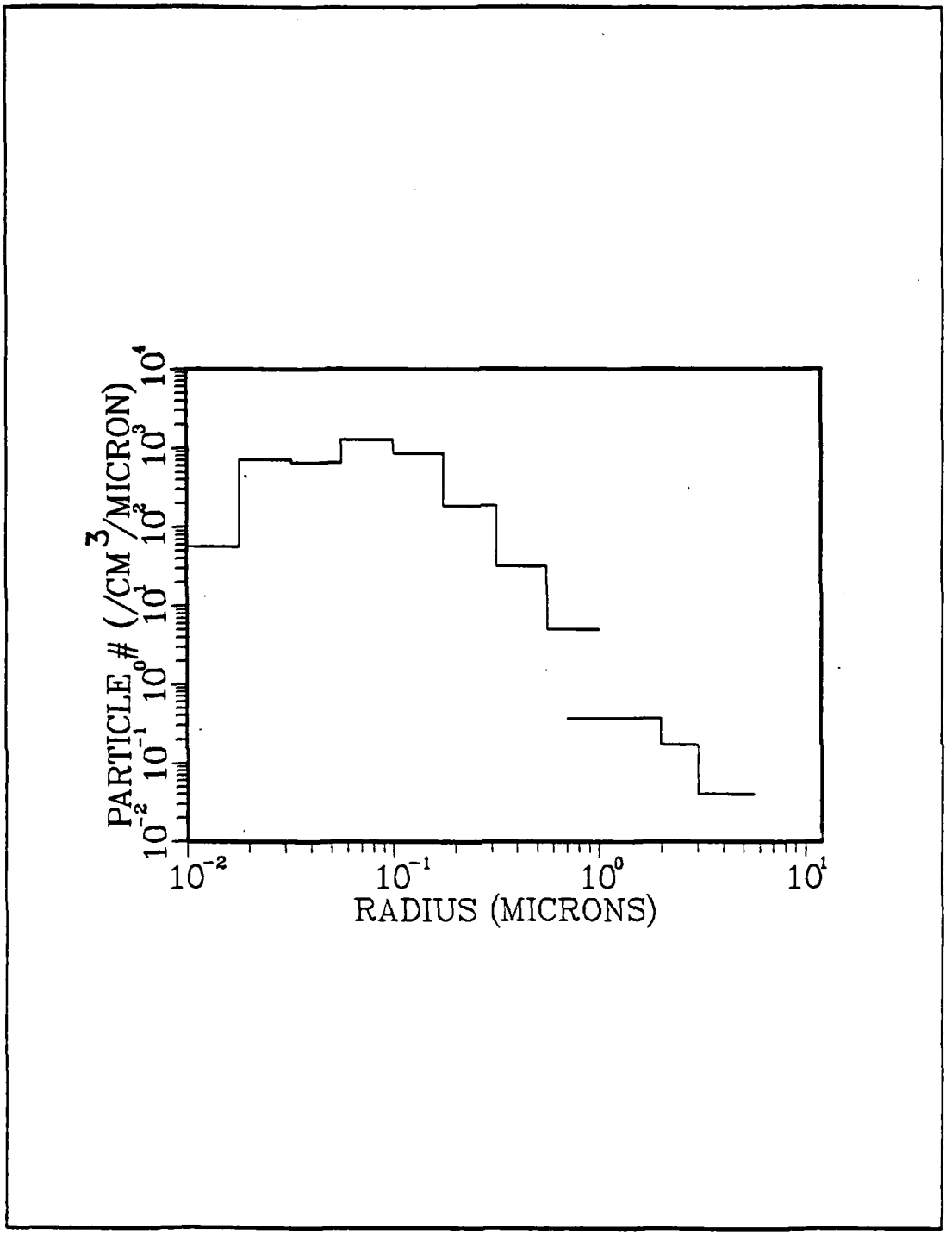

Fig. 4.24 Particle concentrations, 1400 GMT, 23 October 1984.

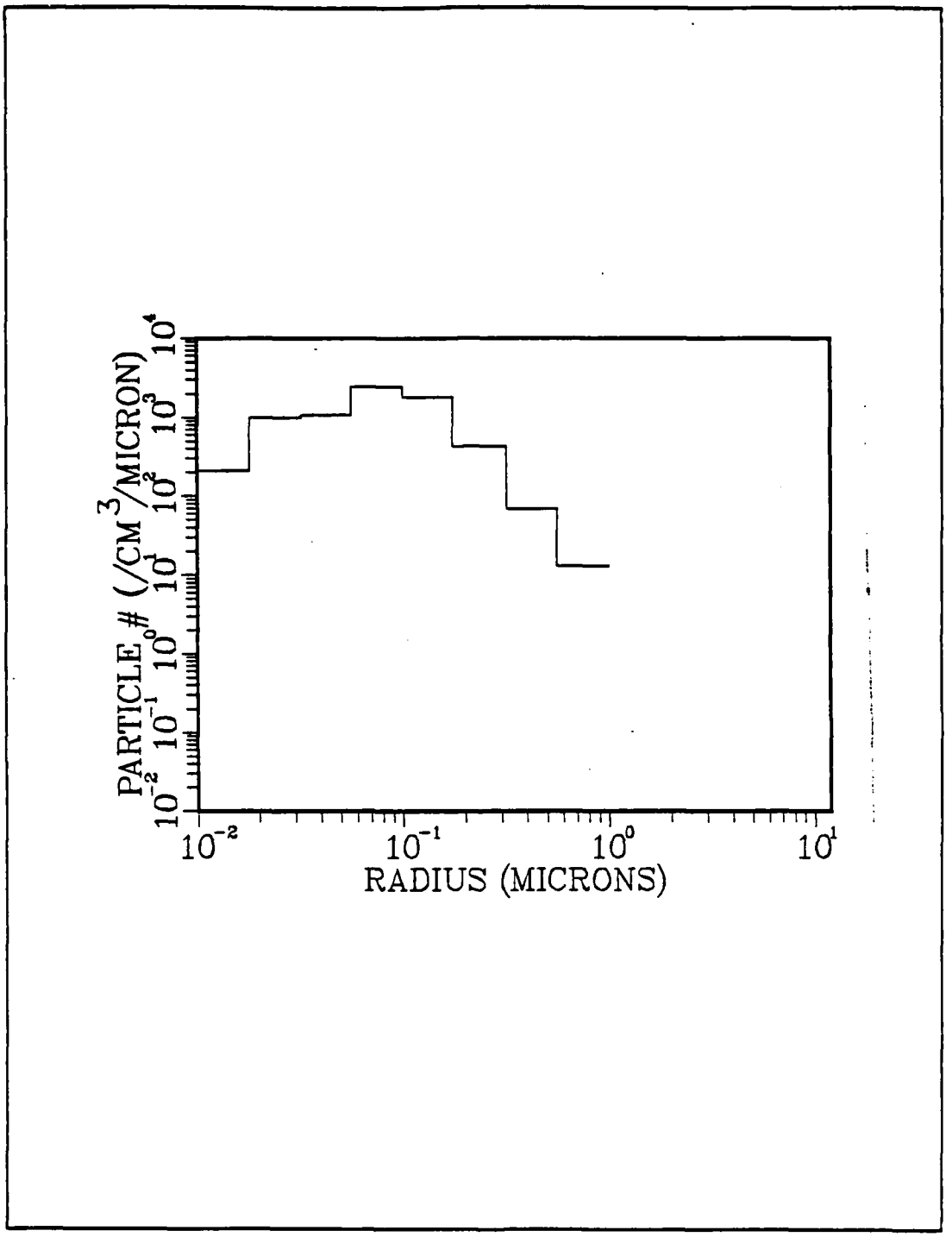

Fig. 4.25 Particle concentrations, 1700 GMT, 23 October 1984.

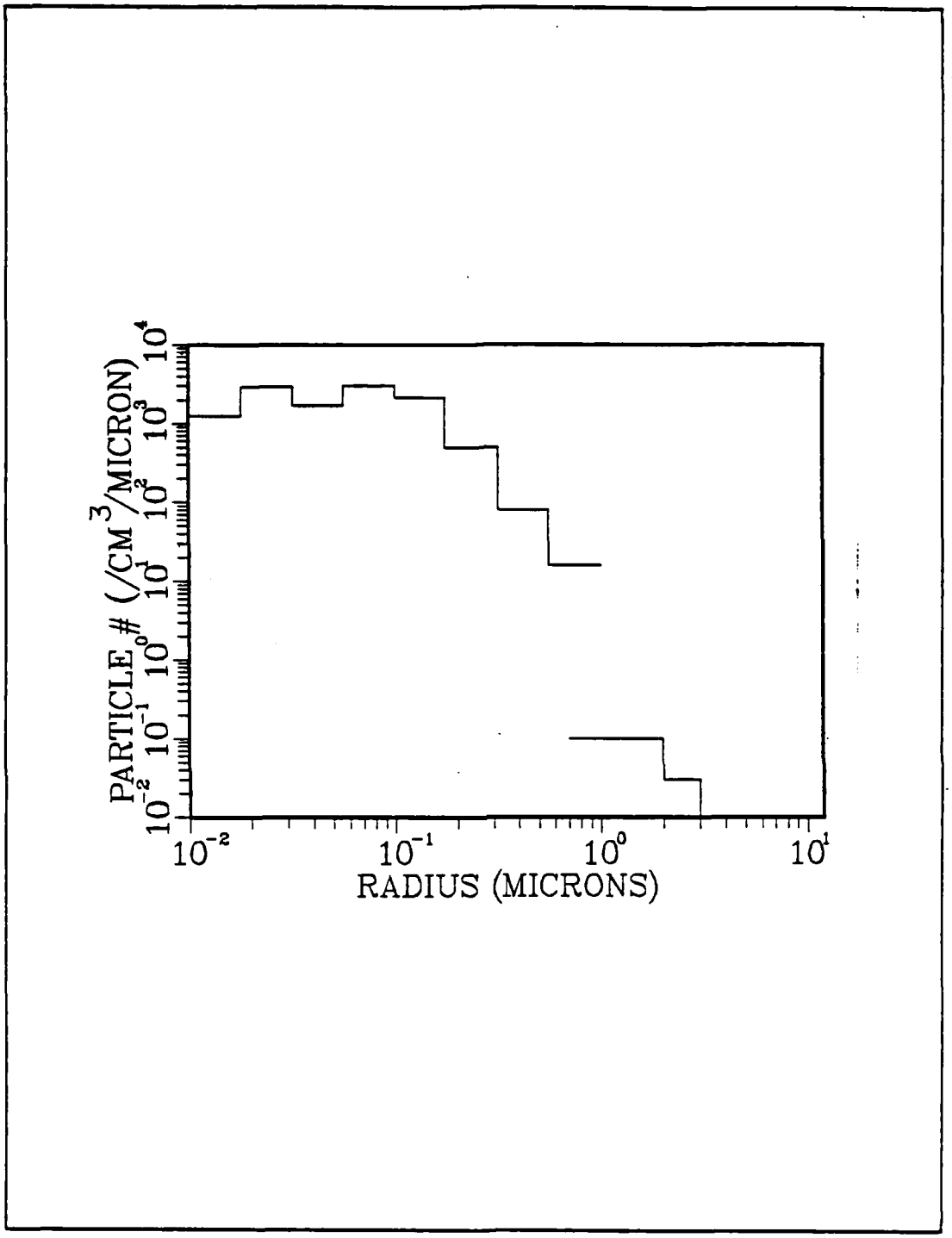

Fig. 4.26 Particle concentrations, 2400 GMT, 23 October 1984.

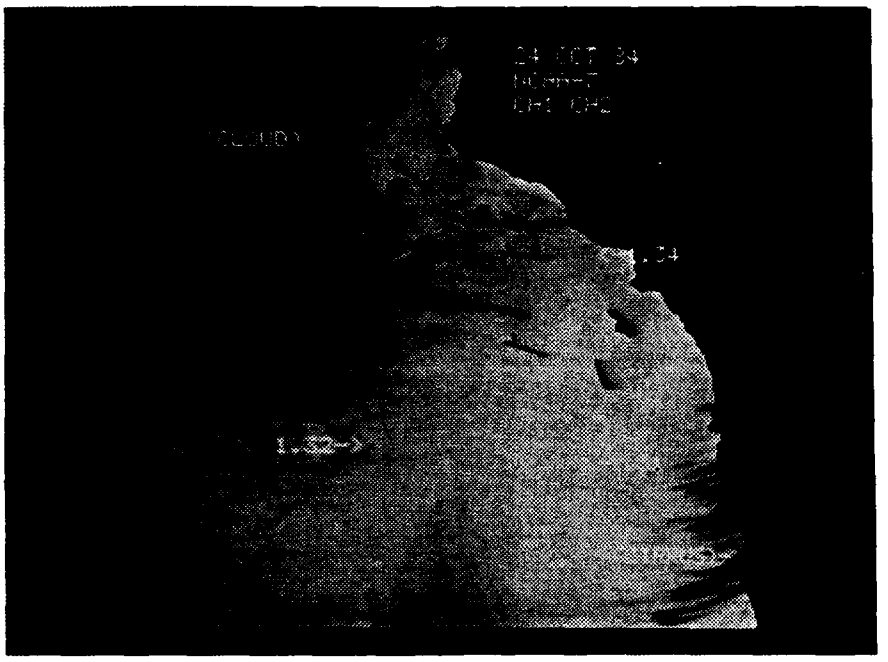

Fig. 4.27 NOAA-7 Channel 1 / Channel 2 ratio image, 2300 GMT, 24 October 1984.

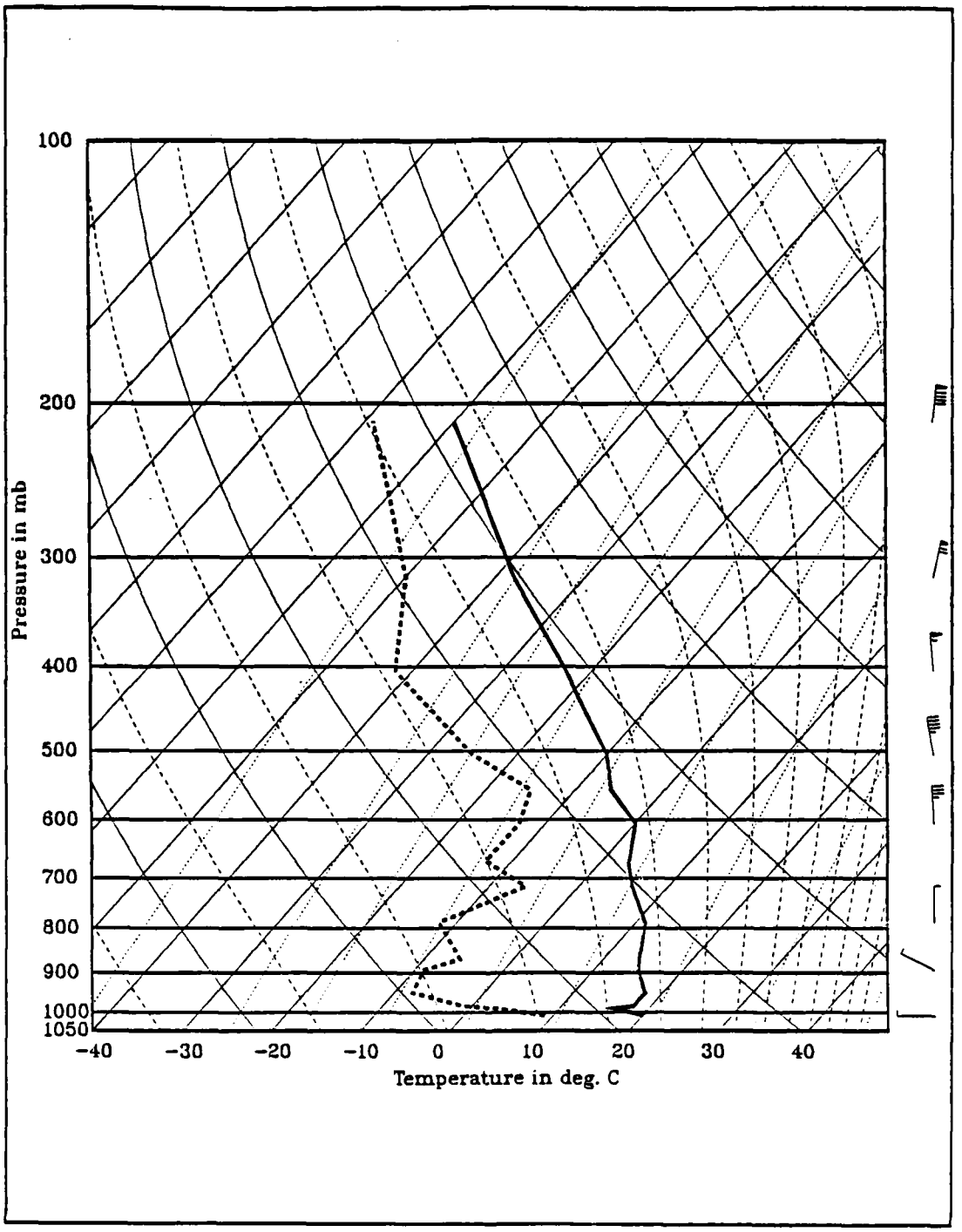

Fig. 4.28 San Nicholas Island rawinsonde observation, 2058 GMT, 24 October 1984.

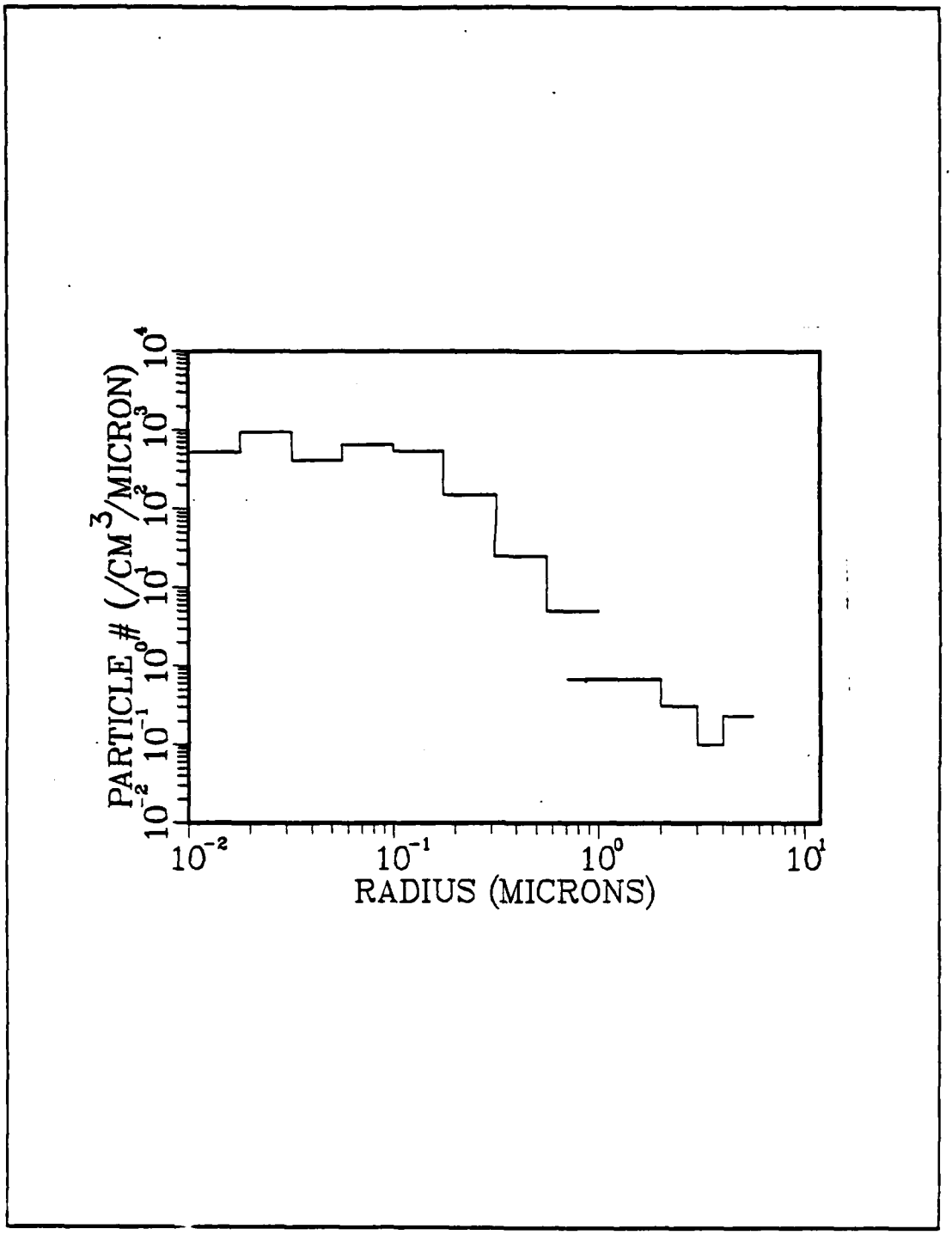

Fig. 4.29 Particle concentrations, 1500 GMT, 24 October 1984.

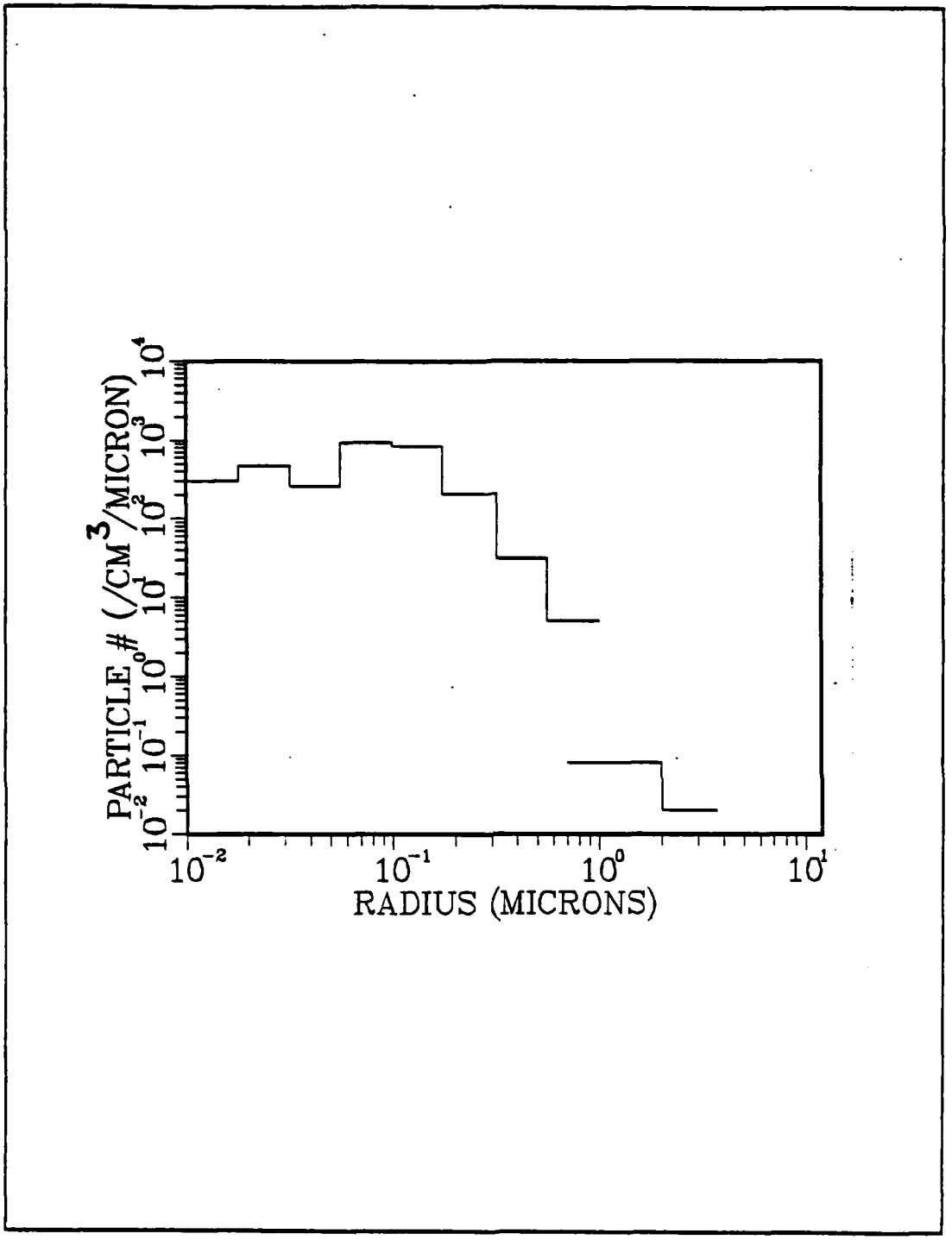

Fig. 4.30 Particle concentrations, 2400 GMT, 24 October 1984.

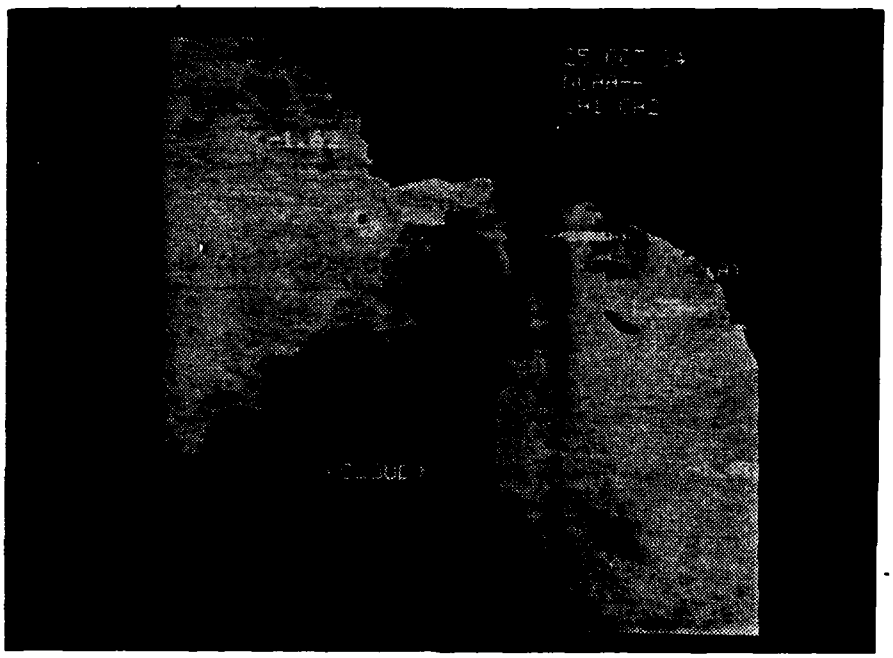

Fig. 4.31 NOAA-6 Channel 1 / Channel 2 ratio image, 1540 GMT, 25 October 1984.

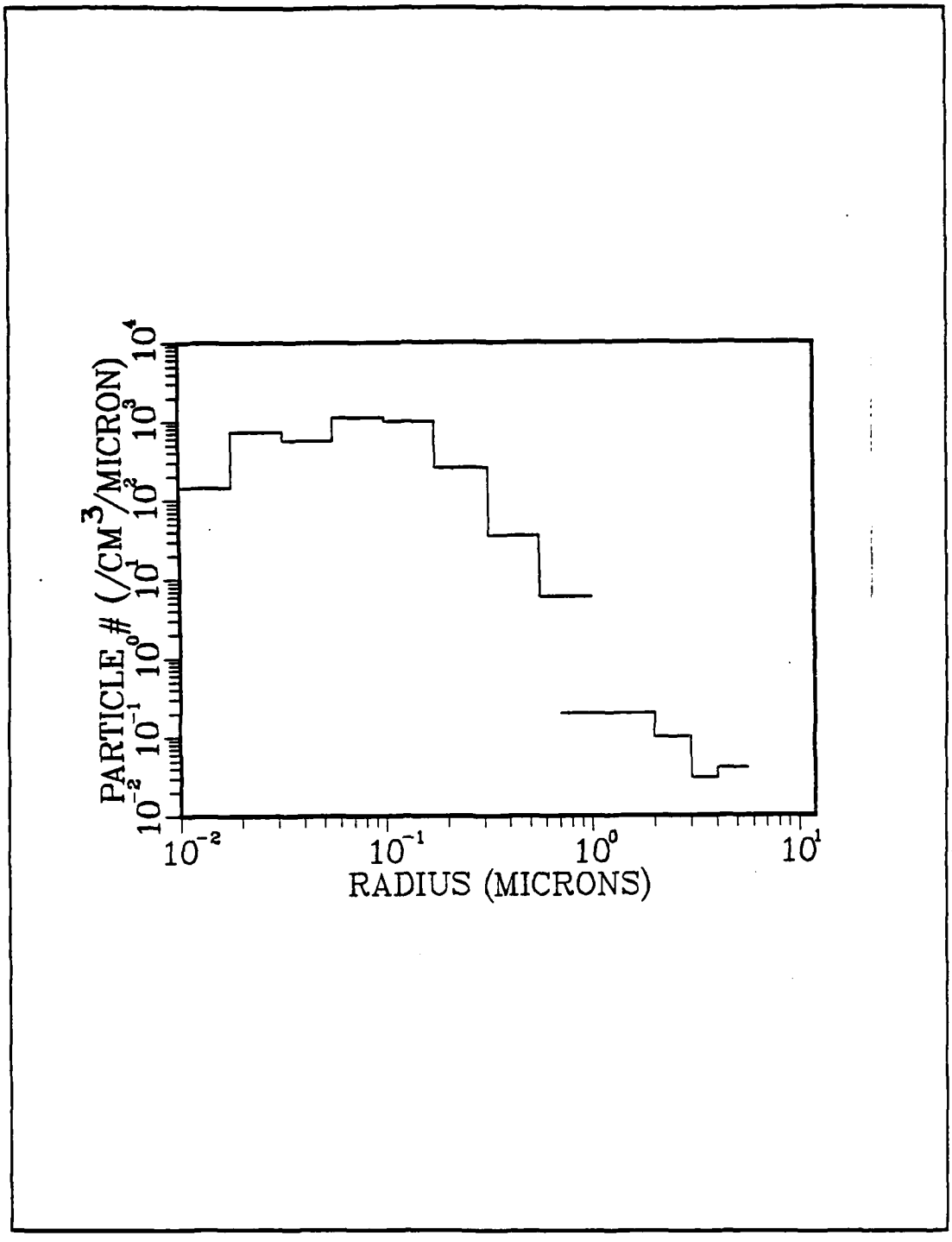

Fig. 4.32 Particle concentrations, 1400 GMT, 25 October 1984.

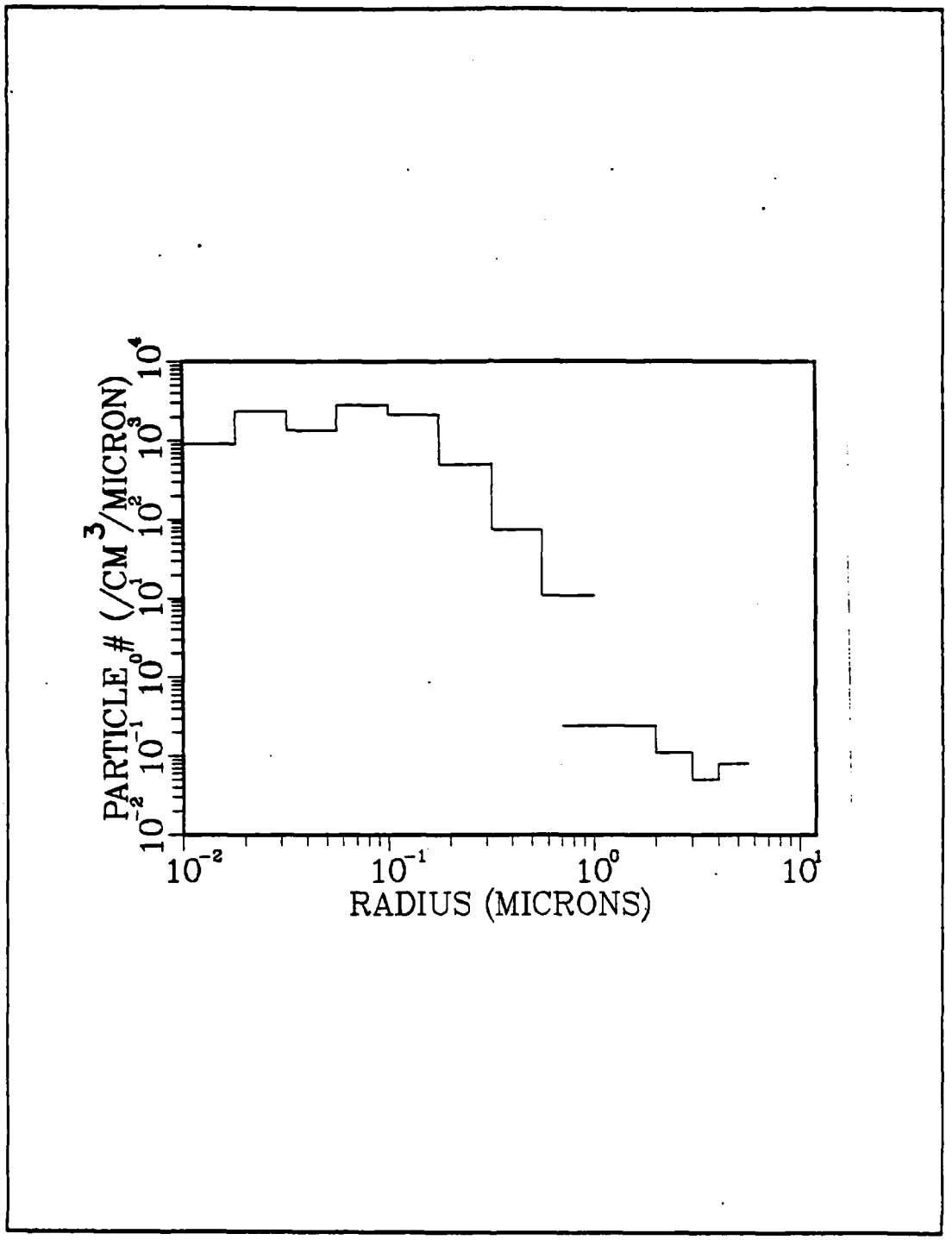

Fig. 4.33 Particle concentrations, 2400 GMT, 25 October 1984.

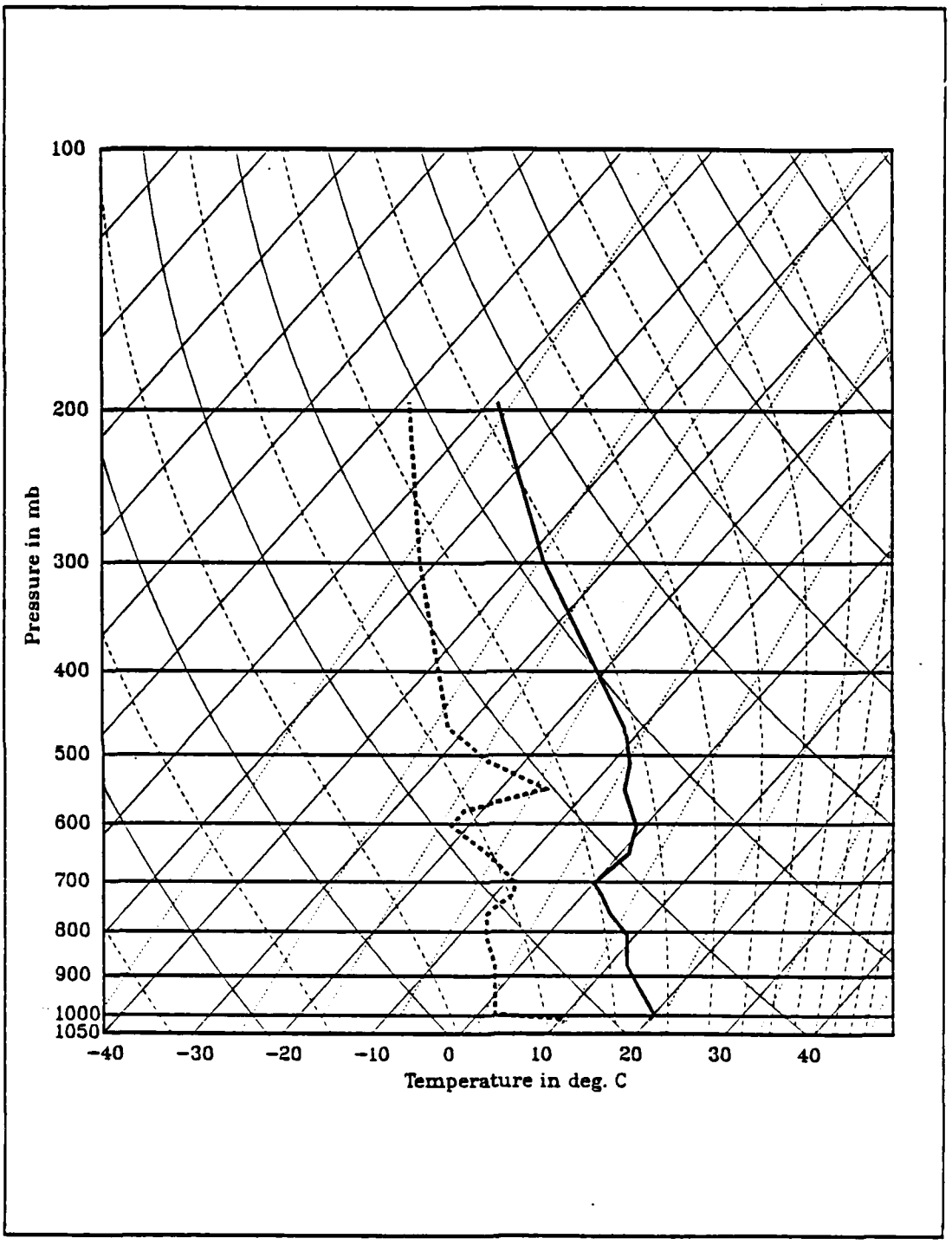

Fig. 4.34 San Nicholas Island rawinsonde observation, 2102 GMT, 25 October 1984.

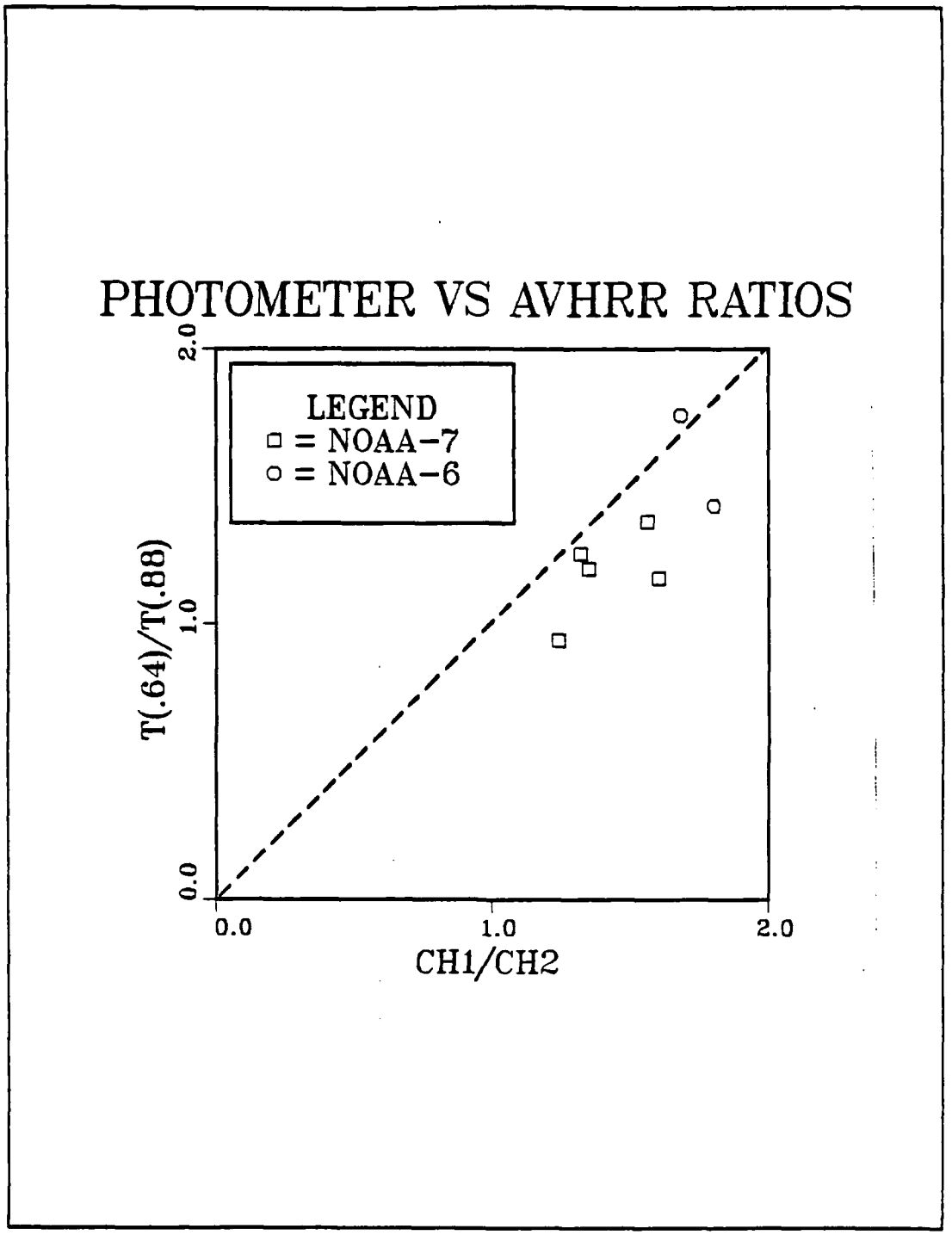

Fig. 4.35 Comparison of aerosol optical depth ratios with AVHRR channel 1 and channel 2 brightness measurement ratios.

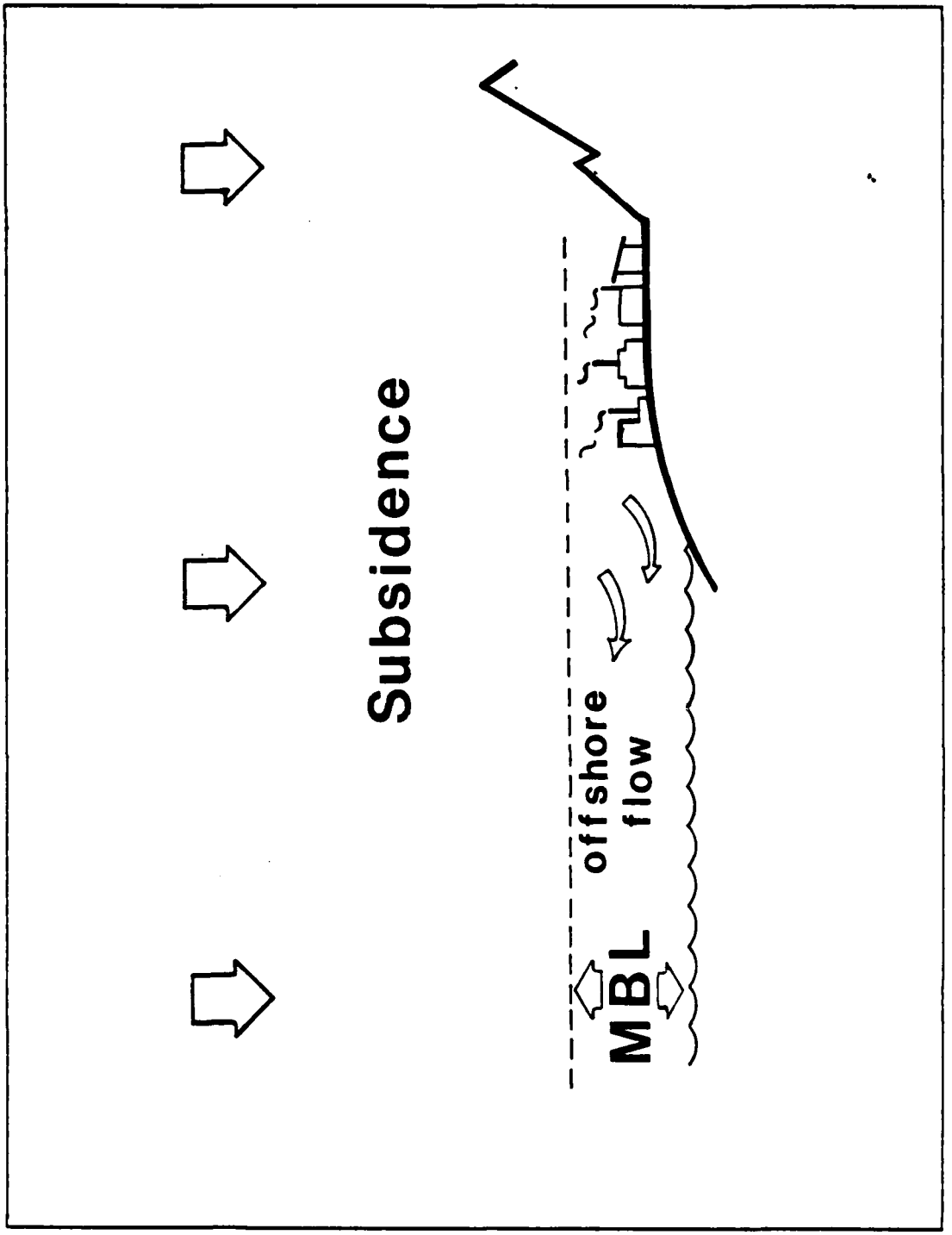

Fig. 4.36 Schematic of a mechanism for trapping and offshore advection of urban particles in the boundary layer.

V. CONCLUSIONS

The ratio values obtained from relating AVHRR channel 1 and channel 2 clearly respond to changes in aerosol particle concentration in the total vertically integrated atmosphere. The ratio values increase as the relative concentration of smaller particles increase, and decrease as the relative concentration of larger particles increase. Thus, the relative horizontal distribution of large vs. small aerosols may be directly inferred. By utilizing appropriate image enhancement techniques, subtle variations in aerosol-induced optical depth changes may be detected.

While horizontal variations in aerosol size concentrations may be readily depicted, determination of the vertical distribution of particles is an inherently more complex problem. Satellite imagery cannot depict vertical variations directly; rather, the atmospheric processes governing aerosol distribution must be understood, and the satellite data interpreted in light of those processes. Durkee (1986) describes a mechanism in which the instability brought on by radiative heating over land allows terrestrial particles to be convectively transported above the boundary layer, where they then spread outwards in the stable region above the marine boundary layer (see Fig. 2.2). In the present study, the absence of significant radiant heating and associated convection over land leads to the establishment of a different aerosol transport mechanism, wherein urban aerosols are trapped within the marine boundary layer (see Fig. 4.36).

The AVHRR channel 1 / channel 2 ratio technique readily depicted this boundary layer marine aerosol transport mechanism. Plumes of low- ratio values responded directly and predictablely to changes in low- level winds and moisture

levels. This technique has application to the monitoring of offshore transport of urban pollutants.

The need for further investigation in this area is evident. The potential sunglint contamination problem noted on certain days of the experiment is one area which needs further study. While sunglint effects may be avoided by selection of appropriate earth-satellite geometry for periods of investigation, the number of usable satellite passes would be decreased. Therefore it is advantageous to develop and incorporate algorithms for elimination of sunglint contamination into the ratio processing technique.

Further investigation into the vertical distribution of aerosols and their relation to the ratio technique is also required. It is emphasised that all particle concentration data examined in this study were acquired at the surface on San Nicholas Island. Thus, inferences as to the vertical distribution of aerosols are tentative. It is proposed to apply the red / near-infrared image ratio process to additional data sets containing vertical particle distribution within and above the marine boundary layer as in Durkee (1986). Such a study may help to refine the construction of regional aerosol distribution and transport models, which will enhance the application of remote sensing techniques to understanding of atmospheric aerosol processes.

LIST OF REFERENCES

Durkee, P.A., 1986: "Aerosol characteristics inferred from dual- wavelenth radiance measurements", conditionally accepted for publication in J. Geophys. Res.

Durkee, P.A., D.R. Jensen, E.E. Hindman and T.H. Vonder Haar, 1986: "The relationship between marine aerosol particles and satellite- detected radiance", J. Geophys. Res., 91, 4063.

Griggs, M., 1983, "Satellite measurements of tropospheric aerosols," Adv. Space Res., 2, 109-118.

Lauritson, L., G.J. Nelson, and F.W. Porton, 1979: Data extraction and calibration of TIROS-N/NOAA radiometers. NOAA Tech. Mem. NESS-107.

Mack, E.J., C.W. Rogers, B.J. Wattle and J.T. Hanley, 1985: Optical depth and aerosol characteristics on San Nicholas Island during the SNI-84 Vertical Structure Experiment, Interim Report, November 1985, Calspan Corporation, Buffalo, New York.

McClintock, M., A. McLellan, and L.A. Sromovsky, 1971: Satellite measurements of spectral turbidity and albedo, and their rates of change. Report to the Environmental Protection Agency, UWI-SSEC-GAP-71-003, July 30, 1971.

Shettle, E.P., and R.W. Fenn, 1979: Models for the aerosols of the lower atmosphere and the effects of humidity variations on their optical properties. AFGL-TR-79-0214, Air Force Geophysics Laboratories, Hanscom AFB, MA.

Yue, G.K., and A. Deepak, 1983: "Retrieval of stratospheric aerosol distribution from atmospheric extiction of solar radiation at two wavelengths", Applied Optics, 22, 1639-1645.

INITIAL DISTRIBUTION LIST

		No. Copies
1.	Defense Technical Information Center Cameron Station Alexandria, Virginia 22304-6145	2
2.	Library, Code 0142 Naval Postgraduate School Monterey, California 94943-5002	2
3.	Chairman (Code 68Mr) Department of Oceanography Naval Postgraduate School Monterey, California 93943-5000	1
4.	Chairman (Code 63Rd) Department of Meteorology Naval Postgraduate School Monterey, California 93943-5000	1
5.	Prof. P.A. Durkee, (Code 63De) Naval Postgraduate School Monterey, California 93943-5000	15
6.	Director Naval Oceanography Division Naval Observatory 34th and Massachusetts Avenue NW Washington, DC 20390	1
7.	Commander Naval Oceanography Command NSTL Station Bay St. Louis, MS 39522	1
8.	Commanding Officer Naval Oceanographic Office NSTL Station Bay St. Louis, MS 39522	1
9.	Commanding Officer Fleet Numerical Oceanography Center Monterey, CA 93940-5005	1
10.	Commanding Officer Naval Ocean Research and Development Activity NSTL Station Bay St.Louis, MS 39522	1
11.	Commanding Officer Naval Environmental Prediction Research Facility Monterey, CA 93943	1
12.	Chairman, Oceanography Department U.S. Naval Academy Annapolis, MD 21402	1
13.	Chief of Naval Research 800 N. Quincy Street Arlington, VA 22217	1

14. Office of Naval Research (Code 420) 1
Naval Ocean Research and Development Activity
800 N. Quincy Street
Arlington, VA 22217

15. Scientific Liaison Office 1
Office of Naval Research
Scripps Institution of Oceanography
La Jolla, CA 92037

16. Library 1
Scripps Institution of Oceanography
La Jolla, CA 92037

17. Library 1
Department of Oceanography
University of Washington
Seattle, WA 98105

18. Library 1
CICESE
P.O.Box 4803
San Ysidro, CA 92073

19. Library 1
School of Oceanography
Oregon State University
Corvallis, OR 97331

20. Commander 1
Oceanographic Systems Pacific
Box 1390
Pearl Harbor, HI 96860

21. Chief, Ocean Services Division 1
National Oceanic and Atmospheric Administration
8060 Thirteenth Street
Silver Springs, MD 20910

END

DTIC

6-86